AN ABSTRACT OF THE THESIS OF

Jong Soo Cho for the degree of Doctor of Philosophy in Chemical Engineering presented on November 19, 1987.

Title : Gas Absorption in a Countercurrent Packed Tower:
(1) Absorption with Simultaneous Chemical Reaction
(2) Absorption into Varying Viscous Solutions

Abstract approved : Signature redacted for privacy.
Charles E. Wicks

The surface renewal rate from Danckwerts' theory and the effective interfacial area between gas and liquid per unit packing volume in a packed absorption tower were evaluated for the absorption of carbon dioxide into carbonate/bicarbonate buffer solution accompanied by a pseudo-first order chemical reaction. The rate of chemical reaction in the liquid phase was controlled by varying the buffer ratios.

A small absorption tower was constructed, which had a packing section, 30 cm high with 10.2 cm inside diameter. Two kinds of packing, ½-inch Raschig ring for one part of the experiment and ½-inch Berl saddle for the other part of the experiment, were used in the investigation. Sodium carbonate/bicarbonate buffer solutions, with buffer ratios varying from 0.4 to 3.0, were used.

Glycerine-water solutions were also used to

investigate the effect of density and viscosity on the physical absorption of carbon dioxide; the content of glycerine varied from 0 to 40 % wt. Pure carbon dioxide was used to eliminate the gas side resistance in the mass transfer operation.

The results of this investigation suggested the following conclusions:

1. The surface renewal rate, s, and the effective interfacial area per unit packing volume, a, for each packing can be expressed as functions of Reynolds Number of the liquid flow.

2. The comparison of values from this study with those of Danckwerts showed discrepancies; these discrepancies could be due to different flow patterns, packing densities, and the apparently more uniform distribution of liquid over the packing.

3. The mass transfer coefficient for physical absorption into glycerine solution was expressed as a function of Reynolds number and Schmidt number.

4. The mass transfer coefficient calculated from Danckwerts' model equation, $k_L*a = a*\sqrt{Ds}$, for absorption of carbon dioxide into water seemed to be larger than those measured in this experiment.

Gas Absorption in a Countercurrent Packed Tower: (1) Absorption with Simultaneous Chemical Reaction (2) Absorption into Varying Viscous Solutions

by

Jong Soo Cho

A Thesis

Submitted to

Oregon State University

in partial fulfillment of
the requirements for the
degree of

Doctor of Philosophy

Completed November 19, 1987
Commencement June, 1988

ACKNOWLEDGEMENT

The author wishes to extend his grateful appreciation to the following:

Dr. Charles E. Wicks, professor and chairman of Chemical Engineering department, for his very generous assistance throughout the duration of this study.

Department of Chemical Engineering for its financial assistance and allowance of the use of its facilities.

Nick, for his help in construction of experimental apparatus.

And finally his parents, who deserve much of the credit for the completion of this study.

Table of Contents

List of Figures

List of Tables

GAS ABSORPTION IN A COUNTERCURRENT PACKED TOWER: (1) ABSORPTION WITH SIMULTANEOUS CHEMICAL REACTION (2) ABSORPTION INTO VARYING VISCOUS SOLUTIONS

Introduction

The absorption of a gas component into a liquid phase is an important unit operation in chemical industries. The object of this operation is either the elimination of an undesired component from a gas mixture or the production of desired products by the liquid phase reaction between liquid component and gas component. The removal of some components is very important especially in pollution control, like the removal of CO_2, SO_2, and H_2S from the flue gas. The production of desired products by gas-liquid reaction includes the nitrogenation, oxidation, or hydrogenation of organic compounds. To perform these processes properly, whether they are removals of gas components or absorptions for reaction, the mass transfer mechanism between gas and liquid phases must be thoroughly understood.

There are several types of equipment available for absorption process. Among them, the packed tower is a very popular one for its large capacity resulting from the enlarged contacting area between gas and liquid phases. To design a packed tower properly for gas absorption, one should collect experimental data. Such data should include

the mass transfer coefficient, the reaction rate and the effective interfacial area inside the column. Several factors determine the mass transfer rate and effective interfacial area. Hydrodynamic factors, such as density, viscosity, gas and liquid flow rates, the shape and the size of packing, and the surface tension of the liquid, are included. Physico-chemical factors include the solubility of the gas component in liquid, the kinetics of reaction, the diffusivities in both phases, etc. All of these factors have some effects on the absorption rate in the column. To make a proper design, all of these factors and their relationships to the mass transfer rate and the effective contacting area must be known.

There has been much research on the mass transfer mechanisms, mass transfer coefficients in gas and liquid phases, and the effective contacting area inside the packed tower. Some of this research consisted of theoretical analyses. Some was based upon experiment. The mass transfer mechanism between gas and liquid phases has been studied theoretically from 1920 to 1960 by several researchers using different models. Some theories give better physical pictures of mass transfer between different phases than others, but the final calculated results are not much different from each other except for some extreme cases.

When it comes to practical design problems, the mass transfer coefficient and the effective interfacial area are the most significant values. Usually, these values have

been obtained by experiment. A common method of obtaining these values involve the experimental evaluation of the absorption or desorption rates into or from a device, which has a known contacting area, to obtain the mass transfer coefficient per unit contacting area. The mass transfer coefficient is then used to determine the effective contacting area for the packing as the final step. From these two experimental steps, one can obtain both the mass transfer coefficient and the effective interfacial area. Usually, the mass transfer capacity per unit volume, which is the product of the mass transfer coefficient and the effective interfacial area per unit volume, is necessary for the design of the tower. This value can be obtained by directly measuring the absorption of gas within a packed tower.

An easy and convenient way of measuring these values was presented by Danckwerts[1]. He presented a random surface renewal model for mass transfer between gas and liquid phases and derived an equation which can be applied to a packed tower operations[2]. He adopted a chemical absorption process with known reaction rates of absorbed component in liquid phase[3]. When the reaction rates are known and can be controlled easily, then the mass transfer coefficient and the effective interfacial area can be obtained simultaneously[4,5]. Danckwerts used a new term, surface renewal rate, to express the mass transfer rate. The values of surface renewal rate, s, are functions of

several factors, including both hydrodynamic and physico-chemical factors. The main goal of this study is to determine the relationships between these factor and the surface renewal rate, s, and verify the method proposed by Danckwerts to obtain the mass transfer coefficient and the effective interfacial area. The mass transfer coefficient for absorption with simultaneous chemical reaction will be compared with those obtained from the physical absorption into solution with various viscosities.

Literature Survey

There has been much research on the subject of mass transfer between gas and liquid with simultaneous chemical reaction. Recently, several books about this subject have been published, where summaries of theories and experiments are included[29,30].

Danckwerts[6] summarized his research on gas-liquid mass transfer based upon his surface renewal theory. He discussed several cases of gas-liquid mass transfer with or without chemical reaction analytically and presented his experimental results.

Shah[7] in his book also discussed gas-liquid absorptions, as well as gas-liquid-solid operations. He discussed many examples and stated results of several kinds of operation processes, both theoretical and experimental.

Recently, a summary of these numerous investigations by various scientists working in this multiphase operation was published in the NATO Advanced Science series in 1983[8]. This book includes not only the basic theory but also the application of absorption to biochemical process and facilitated transport problems. This is a book very recently published on the mass transfer among different phases.

Ramm[9] summarized the works of Eastern Block scientists concerning gas-liquid mass transfer. This book has been translated by an Israeli program for scientific translations in Jerusalem.

These four are excellent introductory books on the theory and practical application of gas-liquid mass transfer with simultaneous chemical reaction.

In the area of practical design, mass transfer coefficients obtained from a bench scale absorption apparatus were commonly used. Among them, Sherwood and Holloway[10] derived the most well-known equation for mass transfer coefficient from desorption and absorption of several kinds of gases into water in packed towers.

Mangers and Ponter[11] extended the equation proposed by Sherwood and Holloway for viscous liquid up to 26 cp. Two correlations applicable for viscous flow were obtained; one for a partially wetted packing and another for a fully wetted one.

The problem of the effective interfacial area has been a very controversial one. Numerous definitions of the effective area were developed and tested for various types of operations. Results varied for each packing and type of operations. The most convenient correlation for the wetted area per unit packing volume is the equation obtained by Onda, et al.[12]. This equation includes the hydrodynamic factors, the surface tension of liquid. The results obtained by several researchers were summarized in a research paper of Semmelbauer[13].

On the surface renewal rate based on Danckwerts' theory, there has been little research except Danckwerts' experiments on certain kind of packing[4,5,6].

Danckwerts and Sharma[14] summarized the method to obtain the mass transfer coefficient and the effective interfacial area using absorption with simultaneous chemical reaction inside the liquid phase when using concurrent flows.

Theoretical Background

Mass transfer between gas and liquid phases without chemical reaction

Mass transfer between two phases has been analyzed by different models including the film model, the penetration model, the surface renewal model, the film-penetration model, the boundary layer model, and the kinetics model. Although each of these models gives a somewhat different physical picture of the process, in many instances the final result for the rate of gas absorption in the presence of a liquid is similar. The film and penetration models are the most widely used models.

The film model was originally proposed by Lewis and Whitman[15]. They assumed that on both sides of the interface, stationary layers or films are formed that separate the interface from the main body of the corresponding phase. They also assumed that in the main body the concentration, c_o, remains constant, and the concentration changes only within the film. The material is transmitted to or from the interface by the steady state molecular diffusion through the layer of the carrier.

The rate of solute transfer across an unit area of interface located at constant x-plane is defined by Fick's law:

$$N\,|_x = - D \frac{dc}{dx}\,|_x \qquad (1)$$

where N is the rate of mass transfer per unit area, c is the concentration of the solute at a distance x below the

surface and D is the mass diffusivity. This equation is integrated over the film of thickness δ to obtain

$$N = \frac{D}{\delta} \left(c^* - c_o \right) \tag{2}$$

where c^* is the saturated concentration at the interface. The convective mass transfer coefficient, k_L, is defined by

$$N = k_L \left(c^* - c_o \right) \tag{3}$$

Comparison between equation(2) and (3) produces the mass transfer coefficient, k_L, for the film model

$$k_L = \frac{D}{\delta} \tag{4}$$

The film model is based on simplistic assumptions and does not take into account the influence that the motion of the phases has along the interface on the transmission of material. This model does not provide a quantitative relationship to determine the thickness of films.

The penetration models are based upon the transient mass transfer across the interface. A mass balance for the solute over a small elemental volume of uniform cross-sectional area between x and x+dx for a given time interval, dt, gives

$$\frac{\partial c}{\partial t} = D \frac{\partial^2 c}{\partial x^2} \tag{5}$$

Common boundary conditions often encountered are saturated concentration of the solute at the interface,

$$c=c^* \quad \text{at } x=0,\ t>0 \tag{5a}$$

uniform initial concentration of the solute within the phase,

$$c=c_o \quad \text{at } x>0,\ t\leq 0 \tag{5b}$$

and constant concentration of the solute at a great depth into the phase,

$$c=c_o \quad \text{at } x=\infty, \ t>0 \tag{5c}$$

The solution of equation(5) with the given boundary conditions yields

$$\frac{c - c_o}{c^* - c_o} = \text{erfc} \left(\frac{x}{2\sqrt{Dt}} \right) \tag{6}$$

where erfc z represents the complimentary error function of z; this function equals

$$\text{erfc } z = 1 - \frac{2}{\pi} \int_0^z e^{-\sigma^2} d\sigma \tag{7}$$

The instantaneous rate of mass transfer per unit area at the interface, x=0, is obtained by differentiating equation(6) and inserting the gradient of the concentration into equation(1); this yields

$$N \Big|_{x=0} = - D \frac{dc}{dx} \Big|_{x=0} = \sqrt{\frac{D}{\pi t}} (c^* - c_o) \tag{8}$$

The average rate of mass transfer is evaluated by

$$N_{ave} \Big|_{x=0} = \frac{\int_0^{t_{exp}} N \Big|_{x=0} \, dt}{t_{exp}} \tag{9}$$

where t_{exp} is the total exposure time for the transfer of the solute into the liquid phase; this result is

$$N_{ave} \Big|_{x=0} = 2 \sqrt{\frac{D}{\pi t_{exp}}} (c^* - c_o) \tag{10}$$

The mass transfer coefficient, k_L, is defined by

$$N_{ave} = k_L (c^* - c_o) \tag{3}$$

Comparison between equation(3) and (10) reveals

$$k_L = 2 \sqrt{\frac{D}{\pi t_{exp}}} \tag{11}$$

This is Higbie's penetration model[16] for mass transfer. Danckwerts[2] proposed the random surface renewal model which involved a surface age distribution function, ø(t); this function presented the probability that any element of the surface area will be exposed for a time t before that element is replaced by a fresh eddy from the bulk of the fluid. According to this concept, the average mass transfer rate becomes

$$N_{ave} = \int_0^{\infty} (N)_{ins}\, \phi(t)\, dt \qquad (12)$$

where N_{ins} is the instantaneous rate of transfer of solute as defined by equation(8). Danckwerts proposed the following distribution function

$$\phi(t) = s\, e^{-st} \qquad (13)$$

where s is the fractional rate of renewal of the area exposed for mass transfer. Upon substitution of equation(8) and equation(13) and integration, the following equation is obtained

$$N_{ave} = (c^* - c_o)\sqrt{Ds} \qquad (14)$$

The liquid side mass transfer coefficient can be expressed by the Danckwerts' model by

$$k_L = \sqrt{D\, s} \qquad (15)$$

The fractional rate of surface renewal, s, is an unpredictable quantity which must be experimentally measured for a given system.

By considering hydrodynamics and convective diffusion together, the boundary layer model has been discussed in the papers of Levich[17], Sherwood[18], and

Ruckenstein[19]. Levich discussed a viscous boundary layer in which turbulent flow does not cease abruptly but is gradually weakened as the interface is approached. Ruckenstein believed that the laminar boundary layer is formed over a short sector only. After the solute passes the sector it mixes with the main body. This model is similar to the renewal model. The thickness of the diffusion layer z_o is less than the thickness of the viscous boundary layer, z', i.e.,

$$z_o = z' (Sc)^{-n} \tag{16}$$

where Sc is the Schmidt number. According to Levich[17], n=0.5 for the liquid-gas interface and n=0.33 for the Ruckenstein[19] model.

Kishinevskii[20], in the same way as Higbie, considered the period of contact to be constant. However, in contrast to other researchers, he believed that the transmission of material takes place not only by molecular diffusion but also by eddy diffusion. Hence the sum of the coefficients of molecular and eddy diffusion, called the effective diffusion coefficient can be used in place of molecular diffusion coefficient.

Toor and Marcello[21] stated that both the film and the renewal model are extreme cases of a more general mechanism of mass transfer. They assumed that the contact points of the surface have a certain thickness and that mass transfer to new points of contact fits the renewal model, and, at the same time, mass transfer to the old

points of contact fits the film model.

Mass transfer with a first order chemical reaction

When the dissolved gas reacts with a component in the liquid the mass balance for the dissolved gas component over a small elemental volume of uniform cross-sectional area is

$$\frac{\partial c}{\partial t} = D \frac{\partial^2 c}{\partial x^2} + r_c(x,t) \tag{17}$$

where $r_c(x,t)$ is the reaction rate per unit volume of liquid at which the reaction destroys the solute at time t and at a distance x below the surface. This rate in general depends on the local concentration of the gas component and of any other component with which it reacts. Analytical or numerical solutions of the diffusion-reaction equations are available for a number of cases[6].

In this study, only the first order irreversible reaction case will be treated. When there is a first-order irreversible reaction in liquid phase with respect to dissolved gas component, the reaction rate, $r_c(x,t)$, is

$$r_c = - k_1 c \tag{18}$$

The general differential equation for mass transfer in one-direction is

$$\frac{\partial c}{\partial t} = D \frac{\partial^2 c}{\partial x^2} - k_1 c \tag{19}$$

with the boundary conditions

$$c = c^* \text{ at } x = 0, \ t > 0 \tag{19a}$$

$$c = 0 \text{ at } x > 0, \ t \leq 0 \tag{19b}$$

$$c = 0 \text{ at } x = \infty, \ t > 0 \tag{19c}$$

The solution of this equation is

$$\frac{c}{c^*} = \frac{I}{2} e^{-x\sqrt{k_1/D}} \operatorname{erfc}\left[\frac{x}{2\sqrt{Dt}} - \sqrt{k_1 t}\right] + \frac{I}{2} e^{x\sqrt{k_1/D}} \operatorname{erfc}\left[\frac{x}{2\sqrt{Dt}} + \sqrt{k_1 t}\right] \quad (20)$$

From the definition of the rate of solute transfer at the interface, x=0, equation(20) gives

$$N|_{x=0} = c^*\sqrt{Dk_1}\left[\operatorname{erfc}\sqrt{k_1 t} + \frac{e^{-k_1 t}}{\sqrt{\pi k_1 t}}\right] \quad (21)$$

Danckwerts' surface renewal theory can be applied to obtain the average mass transfer rate per unit area at the surface; the result is

$$N_{ave} = \int_0^\infty N_{ins}\, \phi(t)\, dt = c^* \sqrt{D(k_1 + s)} \quad (22)$$

When both sides of equation have been multiplied by the interfacial area per unit volume, a, the gas absorption rate per unit volume can be obtained.

$$N_{ave} * a = c^* a \sqrt{D(k_1 + s)} \quad (23)$$

By squaring of both sides, one obtains

$$(N_{ave} * a)^2 = (c^* a)^2 D k_1 + (c^* a)^2 D s \quad (24)$$

A plot of $(N_{ave} * a)^2$ versus k_1 yields a straight line, with a slope of $(c^* a)^2 D$ and an intercept of $(c^* a)^2 D s$. Then

$$s = \frac{(c^* a)^2 D s}{(c^* a)^2 D} = \frac{\text{intercept of line}}{\text{slope of line}} \quad (25)$$

and

$$a = \frac{\sqrt{(c^* a)^2 D s}}{c^* \sqrt{D s}} \quad (26)$$

Experimental data obtained when a first-order reaction

occurs can be used to predict s,a and the mass transfer coefficient, k_L, from equation(15) if the flow conditions are identical. Comparison of equation (15) and equation(22) with c_o=0 from the boundary condition shows

$$k_L = \sqrt{D(k_1 + s)} \qquad (27)$$

when there is a first-order chemical reaction with respect to gas component in the liquid phase. If the fluid conditions and ionic strength are identical but without chemical reaction, the mass transfer coefficient for absorption without chemical reaction can be obtained from the values obtained in equation(25) and (26) and the definition equation(15).

Absorption of CO_2 into CO_3^{-2}/ HCO_3^- buffer solution

The reaction at which dissolved CO_2 will undergo in the buffer solution is

$$CO_2 + OH^- \rightarrow HCO_3^- \qquad \text{reaction(1)}$$

$$CO_2 + H_2O \rightarrow HCO_3^- + H^+ \qquad \text{reaction(2)}$$

The reaction rate at which the dissolved CO_2 will disappear is

$$r_c = - k_{OH^-} [CO_2][OH^-] \qquad (28)$$

for reaction(1) and

$$r_c = - k_w[CO_2] \qquad (29)$$

for reaction(2). This reaction is so slow that it can be negligible and the total reaction rate can be expressed as equation(28). The second order reaction constant k_{OH^-} was determined by Pinsent, et al.[28] as $4.2X10^{14}\exp(-13250$ cal/RT). The concentration of OH^- in the buffer solution

is given by the expression

$$[OH^-] = \frac{k_w'}{k_2'} \frac{[CO_3^{-2}]}{[HCO_3^-]} \qquad (30)$$

where $k_2' = \frac{[H^+][CO_3^{-2}]}{[HCO_3^-]}$ and $k_w' = [H^+][OH^-]$.

The total reaction displays a pseudo-first order reaction kinetics for the given buffer solution as

$$r_c = - k_1 [CO_2] \qquad (31)$$

where the total pseudo-first order rate constant, k_1, is

$$k_1 \approx k_{OH^-} \frac{k_w'}{k_2'} \frac{[CO_3^{-2}]}{[HCO_3^-]} \qquad (32)$$

The second order reaction rate constant, k_{OH^-}, and the equilibrium constant k_w', k_2' are functions only of temperature. At 25°C, $k_{OH^-}\frac{k_w'}{k_2'}$ is 0.86(sec^{-1})[4]. The plot of the pseudo-first order reaction rate constant k_1 versus $\frac{[CO_3^{-2}]}{[HCO_3^-]}$ buffer ratio is shown in Figure 1. The reaction is followed by

$$HCO_3^- + OH^- \rightleftharpoons CO_3^{-2} + H_2O \qquad \text{reaction(3)}$$

which is a much faster reaction than reaction(1). The overall reaction is

$$CO_2 + 2\ OH^- \rightleftharpoons CO_3^{-2} + H_2O \qquad \text{reaction(4)}$$

<u>Absorption of CO_2 into glycerine-water solution having various viscosity</u>

When carbon dioxide is absorbed into glycerine solution, the rate of absorption can be written as equation(3) with the liquid side mass transfer coefficient k_L. Sherwood and Holloway [10] showed that liquid side mass transfer coefficient for absorption could be represented by the equation

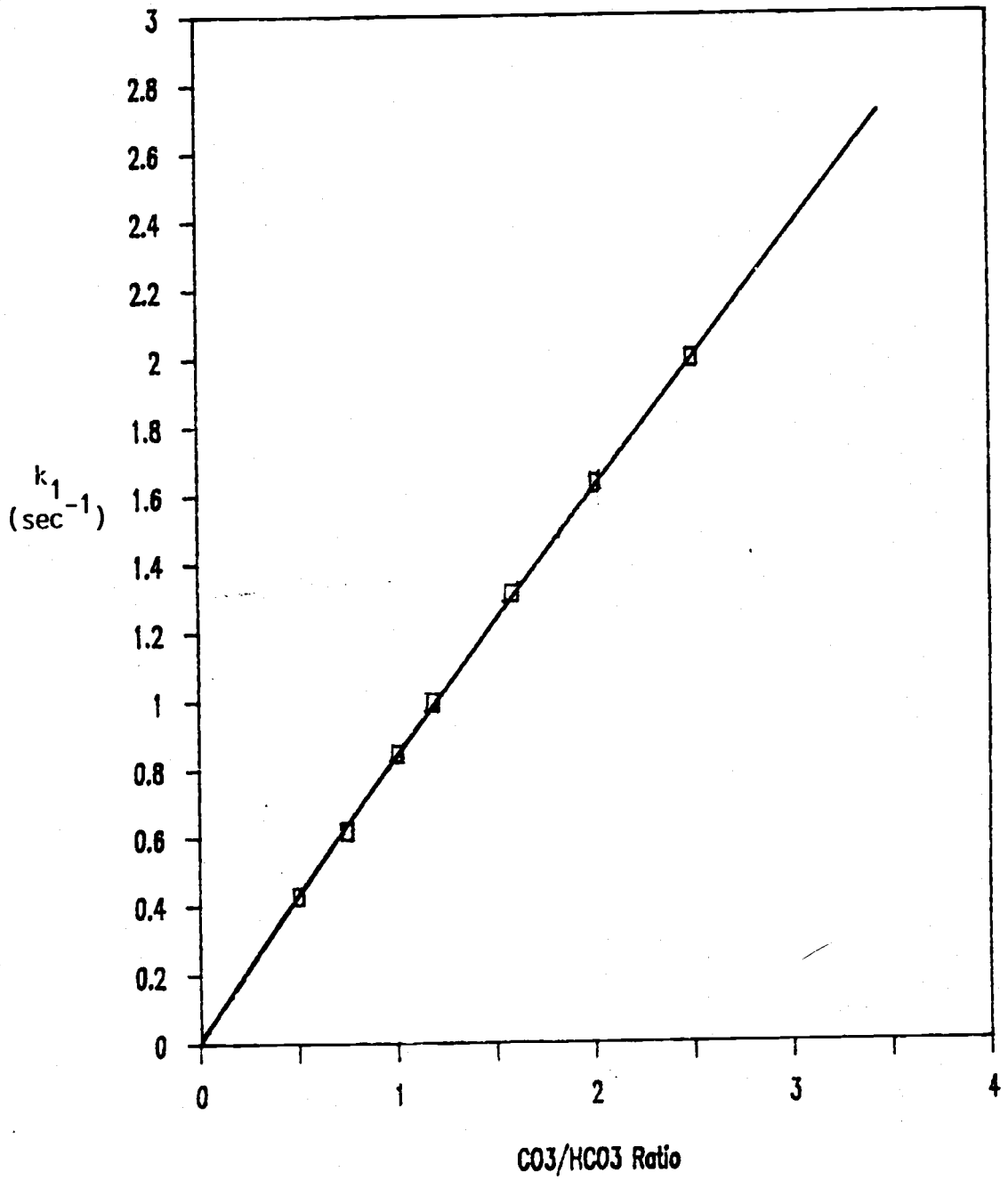

Figure 1 . Buffer ratios and pseudo-first order reaction rate constant k_1

$$\frac{k_L * a}{D} = K\left(\frac{L}{\mu}\right)^m \left(\frac{\mu}{\rho D}\right)^{0.5} \qquad (33)$$

where K and m are constants for a given type and size of packing. This equation indicates that the coefficient is proportional to the square root of the mass diffusivity in agreement with Higbie's theory; the exponent m has been found to vary in value from 0.54 to 0.78. Van Krevelen and Hoftijzer[23] derived an equation for the capacity coefficient, k_L*a, which showed the capacity coefficient was inversely proportional to the kinematic viscosity. Shulman, Ulrich, Proulx and Zimmerman[24] showed that the capacity coefficient was virtually independent of viscosity. This apparent disagreement may have resulted from the fact that the Shulman, et al.'s experiments were confined to very dilute aqueous system with little variation in the viscosity value.

Preparation for Experiment

Apparatus

A schematic diagram of the experimental apparatus is shown in Figure 2. The centerpiece of the absorption system was the packed absorption tower(A). The 10.2 cm I.D. plastic column was 75 cm long with a 30 cm high packed section. It was packed with 1/2-inch ceramic Raschig rings for one part of the experiment and with 1/2-inch nominal size ceramic Berl saddles for another part of the experiment. The packing section was supported by a stainless steel grid mesh. To make the packing section tightly stacked, compressed air was blown up through the packed section filled with water and the packing. The packing was floated for 10 to 15 seconds and then allowed to settle. This process was repeated several times until the packing settled at the lowest position. The same process was done for each packing.

The liquid solution was pumped from the liquid feed reservoir(B), through a rotameter(C) into a liquid distribution head (D) located at the top of column. The 8.9cm diameter distribution head contained 55 1-mm diameter holes uniformly distributed with a 1.4 cm center-to-center triangular arrangement. The head was made of plastic and located just above the top of packed section and provided uniform distribution of liquid into the packing. Figure 3 illustrates the design of the distribution head.

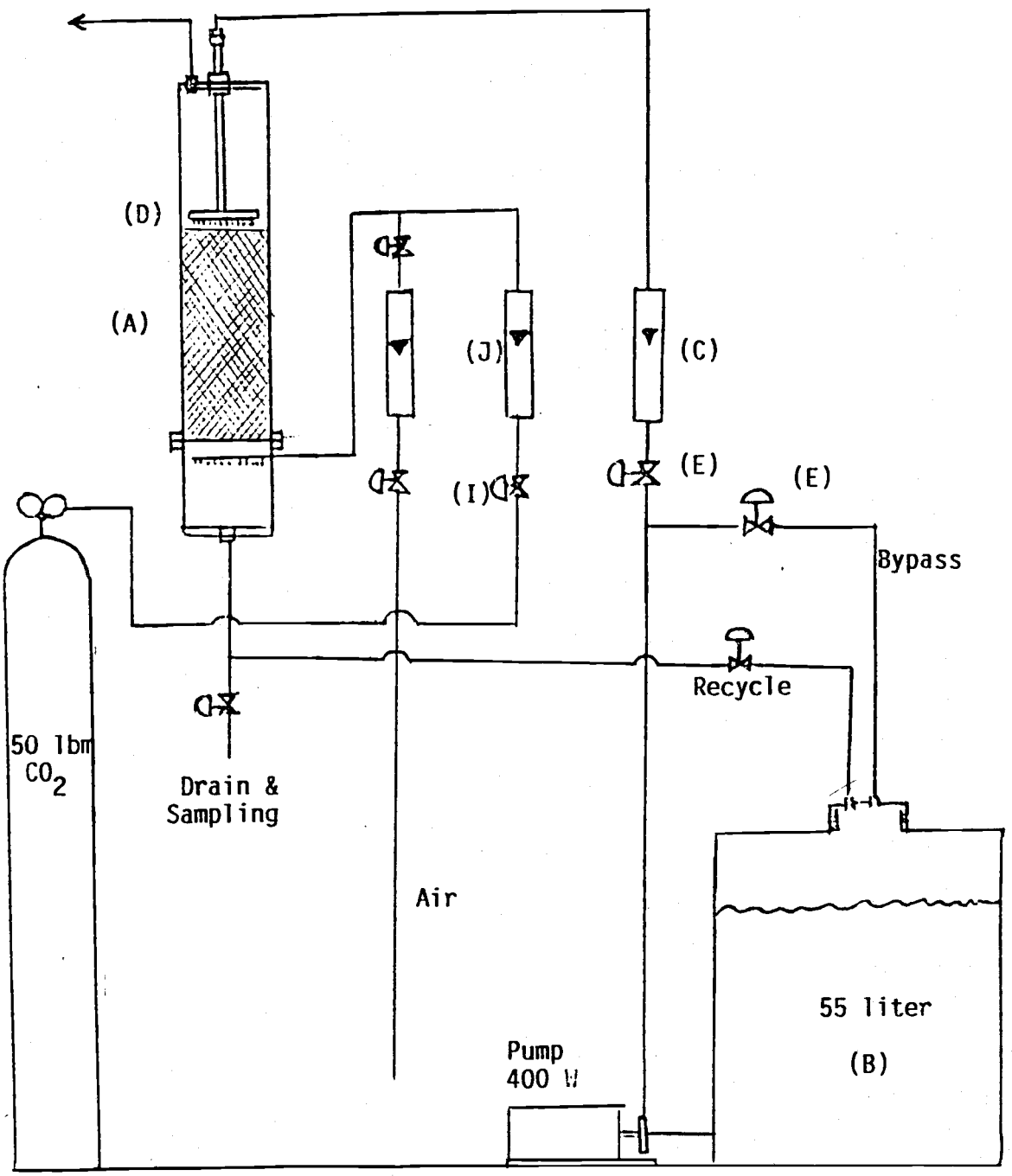

Figure 2. Schematic diagram of experimental apparatus

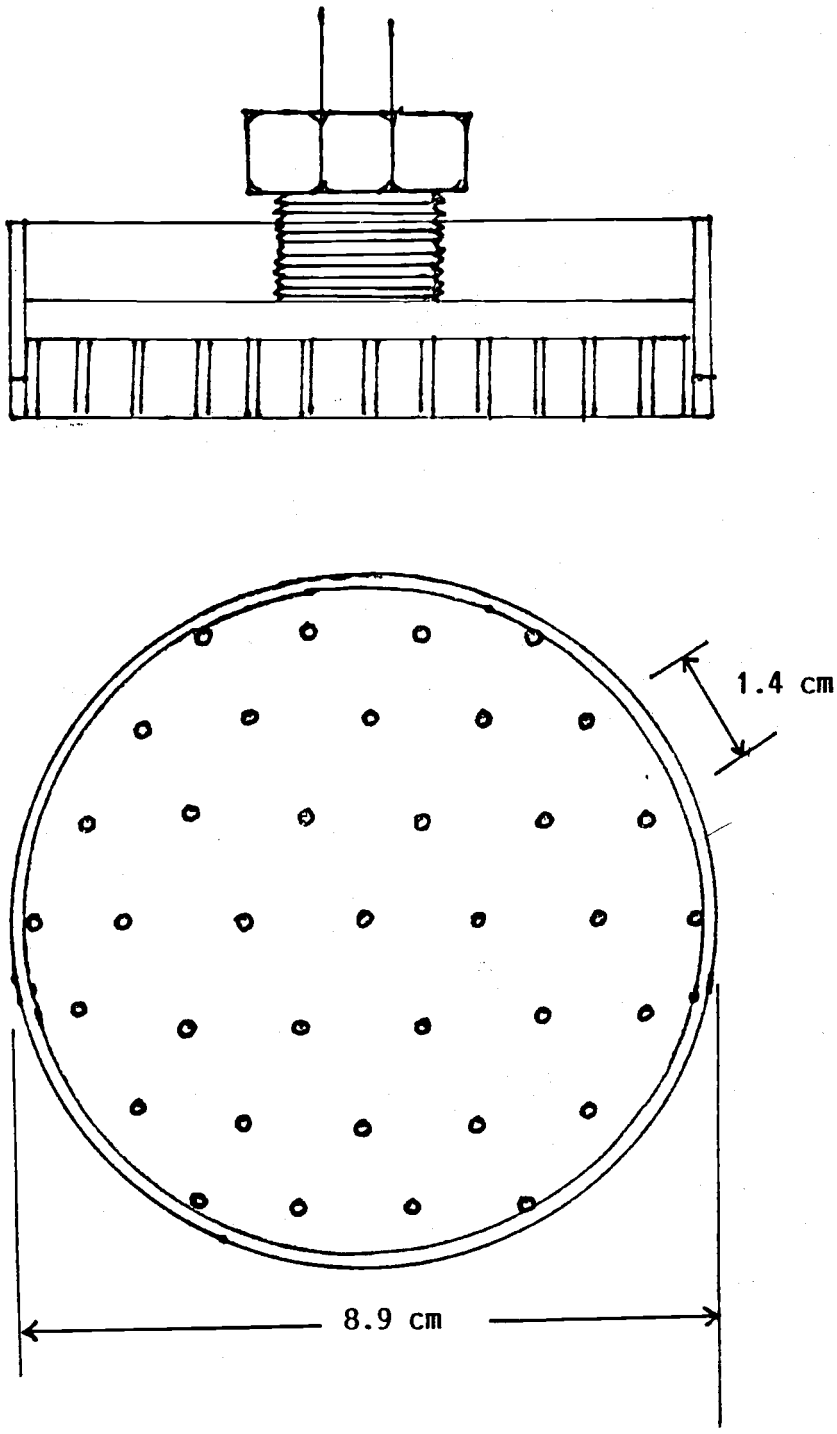

Figure 3. Distribution Head

Two rotary-type 200 watt pumps were connected in series within the liquid pumping system. Nine and a half millimeter o.d. vinyl tubing was used for the liquid piping. The liquid feed rate was controlled by two gate valves(E). One was located in the by-pass flow line immediately behind the pump and the second one was located just ahead of the rotameter in the line to the distribution head. The liquid solution leaving the tower was piped to the drainage. Sample taps were located in both the liquid feed and exit lines.

Two rotameters of different sizes(C) were used in this experiment. One had a 1/4-inch glass tube with a stainless steel spherical float and the other was a 1/2-inch glass tube with a stainless steel bell-shaped float. The former was used for the measurement of the flow rate of the carbonate-bicarbonate buffer solution and the latter for the measurement of the flow rate of glycerine-water solution. Both rotameters were calibrated prior to usage.

Initially, the test results were scattered and showed no reproducibility. This was due to the failure to control the temperature of solution. A large constant temperature water bath was used to control the temperature of the feed solution. A coil of 1/4-inch vinyl tube was immersed into the water bath and the tube was connected to the piping system of liquid feed from the reservoir. The liquid feed solution pumped from the reservoir, passed through the tubes in the water bath before entering the packing

section. The temperature of the liquid feed was controlled at 25 ± 0.5°C. The water of the heating bath was heated by steam introduced into the water directly.

The recycle line from the packed column was used for mixing the solution before it was used to absorb the carbon-dioxide gas. Pure carbon dioxide, CO_2, was supplied to the tower from a 50 lbm pressurized tank(H); the gas pressure was reduced to 15 psia and the gas temperature was maintained at 25°C. The rate of carbon dioxide flow was controlled at 300 cm^3/sec (measured at 1 atm and 25°C) by a needle control valve(I); the flow rate was measured by a CO2 rotameter(J) which was calibrated with air at 25°C.

The pure carbon dioxide gas was introduced into the tower through a gas distributor; this distributor was made of 12.5 cm long horizontal stainless steel pipe of 1.5 mm O.D. Twenty five holes of 1 mm diameter were drilled along the bottom of the tube to distribute the gas uniformly through the packing section and to prevent the solution from flowing into the gas tube.

Calibration of liquid rotameter

The rotameters were calibrated with both water and buffer solutions. Water was pumped through the rotameter and the flow rates were controlled by the gate valves. For a fixed reading, the time required to fill a bucket with water from 15 lbm to 50 lbm was measured. From the density chart at the given temperature, the volumetric flow rate of water was determined. Figure 37 in the Appendix gives a

plot of calibrated reading vs. volumetric flow rate.

The same method was used for the buffer solution. As can be seen in this figure, the volumetric flow rate of the buffer solution was lower for the given reading than the flow rate of water due to its higher kinematic viscosity.

For the glycerine mixture, higher flow rates were required than for the buffer solution. Therefore, a larger capacity rotameter was used. It was calibrated for pure water and 40% glycerine mixtures using the method mentioned above. The plot is illustrated in Figure 38 located in Appendix. As the figure indicates, the difference between the mixtures is quite small. For 10, 20 , and 30% solution mixtures, the flow rate values were interpolated for the given reading.

Calibration of gas rotameter

The gas flow rotameter was calibrated by collecting air which had passed through it. The volume of the air and the time were measured and volumetric flow rates were calculated for the given rotameter readings. Through the whole experiment, the flow rate of carbon dioxide was fixed at 300 cm^3/sec. The calibration curve is in Figure 39 located in Appendix.

Preparation of the buffer solutions

In the phase of the experiment involving the absorption of carbon dioxide accompanied by a first-order reaction, several different buffer solutions were required for the absorbing medium. For each run, twenty-five liters

of solution, containing a given buffer ratio, were consumed; these were made using technical grade sodium carbonate and technical grade sodium bicarbonate. Each prepared solution was analyzed using a acid-base titration analysis. Prior to its use in the experimental run, the prepared solution was stored in a 55-liter, plastic reservoir tank. Five different liquid flow rates were used for each packing and five different buffer solution ratio concentrations were used for each liquid flow rate.

Preparation of the glycerine solution

In the phase of the experiment involving the absorption of carbon dioxide into glycerine-water liquid solutions, five different concentrations were used. These solutions were made by mixing predetermined weights of each component in a 55-liter reservoir tank.

Absorption

The primary objective of this experiment was to determine the relation between the surface renewal rate, s, and the hydrodynamic factors. As pointed out in the theoretical background section, a plot of $(N*a)^2$ versus the first order reaction rate constant, k_1, should give a straight line. From the values of the slope and the intercept of the linear line, the surface renewal rate, s, and interfacial area per unit volume,a, could be evaluated. Kinetics data have been published [22] relating the reaction rate constant for various buffer ratios of carbonate and bicarbonate ions. In the phase of the experiment involving absorption accompanied by a chemical reaction, two different kinds of packing were investigated. For each packing, the absorption process was performed at five different liquid flow rates with a fixed gas flow rate. For each liquid flow rate, six to seven different buffer ratios of CO_3^{-2}/HCO_3^- were used.

Absorption into buffer solutions

The column was packed initially with 1/2-inch ceramic Raschig rings to a depth of 12 inches. The total packing volume was 2460 cm^3 and the total number of packing rings was about 850, which was close to the average packing density in commercial towers. For five different liquid flow rates, 690, 960, 1240, 1380, and 1690 cm^3/min, the absorption was investigated for the Raschig ring packing. The solution was heated to 25°C and temperature was

precisely controlled. The solution was passed through the packing and the CO_2 gas was turned on, flowing into the bottom of packing section, thus flowing a countercurrent to the falling liquid stream. Samples of the exiting fluid were collected for each run and analyzed to determine the amount of carbon dioxide absorbed. Repeated analyses were made to verify the reproducibility of titration analysis. The time of sampling the exit solution from the packed section was 15 to 20 minutes after starting the liquid flow.

The experimental procedures used when the column was packed with 1/2-inch Berl saddles were exactly the same as the procedure used when the column was packed with 1/2-inch Raschig ring.

Absorption into glycerine solutions

The purpose of this experiment was to determine the relationships of Reynolds numbers and mass transfer coefficients for physical absorptions without any chemical reaction. Also, the relationships of viscosity with the mass transfer coefficient were examined, using the data obtained when the tower was packed with 1/2-inch Berl saddles. All of the absorption studies were performed in the same column as that used in the investigation of the absorption in the buffer solutions.

Analysis of CO_2 absorbed in buffer solution

To determine the amount of carbon dioxide absorbed into the buffer solution, two titration procedures were

used. As mentioned in the theoretical background section, carbon dioxide was absorbed and simultaneously reacted in the buffer solution as follows when the ph of solution was greater than 8,

$$CO_2 + OH^- \longrightarrow HCO_3^- + OH^- \qquad \text{reaction(1)}$$

followed by

$$CO_3^{-2} + H_2O \longrightarrow HCO_3^- + OH^- \qquad \text{reaction(5)}$$

The overall reaction is

$$CO_2 + CO_3^{-2} + H_2O \longrightarrow 2HCO_3^- \qquad \text{reaction(6)}$$

The amount of CO_2 which was absorbed and simultaneously reacted in the solution was equal to half of the amount of increase in the bicarbonate concentration within the solution. To determine the amount of concentration change of bicarbonate ion, a titration method was used to evaluate the concentrations in the solution before and after the absorption process. Another titration procedure was used to evaluate the concentration of sodium, Na^+, ion; this concentration was used to evaluate the concentration of CO_3^{-2} ion. The concentration of carbonate ion was obtained to calculate the buffer ratio in the solution.

To perform the titration, two samples of 25 ml solution were collected and put into 200 ml beakers. One of the sample was used for evaluating the total Na^+ ion concentration and the other one for the concentration of bicarbonate ion.

Two or three drops of methyl red indicator were added into one of the samples and the solution was titrated using

1 N HCl solution. Just before arriving at the end point of the titration, the solution was heated in order to evaporate the carbon dioxide in the solution. This evaporation made the color change of the indicator very clear at the end point of the titration. If the volume of the 1 N HCl solution was V_{HCl}, the concentration of Na^+ ion in the solution was determined by

$$[Na^+] = \frac{V_{HCl}}{25} \quad \text{(gmol/liter)} \qquad (34)$$

To the second sample, 25 ml of 1 N NaOH solution was added to convert the total bicarbonate ion to carbonate ion by the following reaction mechanism

$$HCO_3^- + OH^- \longrightarrow CO_3^{-2} + H_2O \qquad \text{reaction(7)}$$

This was an inverse of reaction(5). Then 50 ml of 1 N $BaCl_2$ solution was added to this mixture to precipitate the carbonate ion by following reaction

$$Ba^{+2} + CO_3^{-2} \longrightarrow BaCO_3 \qquad \text{reaction(8)}$$

Barium carbonate has a very small solubility. The hydroxyl ion, OH^-, remaining in the solution was back-titrated using 1 N oxalic acid solution with 2-3 drops of phenolphthalein indicator. When V_{ox} ml of 1 N oxalic acid was added to the solution until it arrived at the end point of the titration, the concentration of HCO_3^- was

$$[HCO_3^-] = 1 - \frac{V_{ox}}{25} \quad \text{(gmol/liter)} \qquad (35)$$

In the mixture of sodium carbonate and sodium bicarbonate, the total concentration of Na^+ ion was

$$[Na^+] = [HCO_3^-] + 2*[CO_3^{-2}] \qquad (36)$$

Therefore, the concentration of carbonate ion in the solution was

$$[CO_3^{-2}] = \frac{1}{2} ([Na^+] - [HCO_3^-]) \quad (37)$$

This titration process was performed for the feed solution prior to its entrance into the packed column and for the solution after it had flowed through the packed column. After determining the initial and final concentrations of bicarbonate ion and carbonate ions, the amount of carbon dioxide absorbed during the absorption process was determined by

$$M = \frac{1}{2} \{ [HCO_3^-]_f - [HCO_3^-]_i \} \quad (\text{gmol/liter}) \quad (38)$$

Analysis of CO_2 absorbed in glycerine-water solution

To determine the concentration of carbon dioxide in glycerine-water solution, the titration process which had been used for analyzing the bicarbonate ion in the buffer solution was adopted. Dissolved carbon dioxide in a glycerine solution reacted with any sodium hydroxide solution added to the solution to produce bicarbonate ion by reaction(1). Furthermore, when an excessive amount of hydroxide solution was added, the reaction(7), which produced carbonate ion, occurred and the entire amount of carbon dioxide in the solution remained as a carbonate ion form in the solution. The concentration of hydroxide ion, which did not react with carbon dioxide, was analyzed by titrating with HCl. The concentration of carbonate ion in the glycerine was around one tenth of that in the buffer solution. Accordingly, 0.1 N HCl, 0.1 N NaOH and 0.1 N

$BaCl_2$ solution were used to accomplish the titration.

Twenty five milliliter of 0.1 N NaOH was added to the sample of 25 ml glycerine-water solution into which carbon dioxide was absorbed to convert the HCO_3^- to CO_3^{-2}. Then 25 ml of 0.1 N $BaCl_2$ solution was added to the mixture to precipitate the barium carbonate. Finally 0.1 N HCl solution was used with 2-3 drops of phenolphthalein indicator for titrating the OH- ion remaining in the solution.

When V_{HCl} was the volume of 0.1 N HCl solution added to the solution at the end point, the concentration of OH- ion was

$$[OH^-] = \frac{0.1 * V_{HCl}}{25} \quad \text{(gmol/liter)} \tag{39}$$

The concentration of CO_2 was

$$[CO_2] = \tfrac{1}{2} * 0.1 * \left(1 - \frac{V_{HCl}}{25} \right) \quad \text{(gmol/liter)} \tag{40}$$

Since there was no carbon dioxide in the feed solution, the amount of carbon dioxide absorbed in the packed column would be

$$M = [CO_2]_f \quad \text{(gmol/liter)} \tag{41}$$

Standardized solution of 1 N NaOH, 1 N HCl, 1 N $BaCl_2$ and 1 N oxalic acid used in the titration process were prepared, using well accepted chemical procedures. The analyzing solutions which were used for titration of glycerine-water solution were made by dilution of 1 N solutions. The procedures used in making the solutions are described in Appendix I.

Calculations

Absorption rate of CO_2 in the buffer solution

From equation(38), the amount of carbon dioxide absorbed in the unit volume of buffer solution during absorption process could be calculated. The multiplication of liquid flow rate to the amount of CO_2 absorbed per unit liquid volume would give the total absorption rate in the packing section during the unit time. Then the rate of absorption in the unit volume of packing could be obtained by dividing the total absorption rate by the total volume of packed section. When V_L was the volumetric flow rate of the buffer solution and V_p was the volume of packed section, the mass transfer rate per unit volume, N*a, would be

$$N*a = M * \frac{V_L}{V_p} * \frac{1}{1000} \quad (gmol/cm^3) \tag{42}$$

From equation(38), the amount of CO_2 absorbed in the buffer solution, M, could be obtained and N*a became

$$N*a = \frac{V_L}{2000*V_p} * \{[HCO_3^-]_f - [HCO_3^-]_i\} (gmol/cm^3) \tag{43}$$

Absorption rate of CO_2 in the glycerine-water solution

The absorption rate of CO_2 in the glycerine-water solution could be calculated from the amount of CO_2 absorbed. When V_L was the liquid flow rate of glycerine-water solution and V_p was the volume of packed section, the absorption rate per unit packing volume, N*a, would be

$$N*a = M * \frac{V_L}{V_p} * \frac{1}{1000} \quad (gmol/cm^3 sec) \tag{44}$$

where M could be obtained from equation(41). The result was

$$N^*a = \frac{V_L}{1000^*V_p} * [HCO_3^-]_f \quad (gmol/cm^3sec) \tag{45}$$

From the definition of mass transfer coefficient per unit packing volume, mass transfer rate per unit volume of packed section was

$$N^*a = k_L^*a \ (c^* - c_o) \tag{46}$$

For the physical absorption in the packed column, the bulk concentration c_o had been changed from $c_o=0$ at the top of the packed section to $c_o=M$ at the bottom of the packed section. Then the average value of mass transfer coefficient was

$$(k_l^*a)_{ave} = \frac{N^*a}{(c^* - c_o)_{ave}} \tag{47}$$

Usually for the packed absorption column, a logarithmic mean value for $(c^* - c_o)$ was used, but for this experiment, the amount of CO_2 absorbed was so small that an arithmetic mean value would not make a serious difference. Accordingly, the mass transfer coefficient became

$$'(k_l^*a)_{ave} = \frac{N^*a}{\frac{1}{2}(c^* - 0) + \frac{1}{2}(c^* - M)}$$

$$= \frac{N^*a}{c^* - \frac{1}{2}M} \tag{48}$$

Results

In the theoretical background section, it was shown that absorption accompanied with a first-order reaction could be explained by the following equation

$$(N*a)^2 = (c^**a)^2Dk_1 + (c^**a)^2sD \qquad (24)$$

According to this equation, a Danckwerts-type plot of $(N*a)^2$ versus the reaction rate constant k_1 should be a straight line, with a slope of $(c^**a)^2D$ and a y-intercept of $(c^**a)^2sD$. At the same ratio of CO_3^{-2}/HCO_3^-, the magnitude of k_1 can be determined from previously established data and the magnitude of $(N*a)^2$ can be obtained from the experimental data reported in this study. The Danckwerts-type plots were drawn in Figures 4 through 8 for the ½-inch Raschig ring and in Figures 9 through 13 for the ½-inch Berl saddle. Straight lines represent the data for all liquid flow rates.

For each plot, after the slope and intercept were determined, the surface renewal rate, s, and the effective interfacial area, a, were determined using the equations

$$s = \frac{(c^*a)^2Ds}{(c^*a)^2D} = \frac{\text{slope}}{\text{intercept}} \qquad (25)$$

and

$$a = \frac{\text{intercept}}{c^*\sqrt{Ds}} \qquad (26)$$

The values of saturated concentration, c^*, and mass diffusivity, D, of carbon dioxide in the solution were obtained from Nysing and Kramer[25] and Hikita, et al.[26] For saturated concentration, c^*, the following equation was used

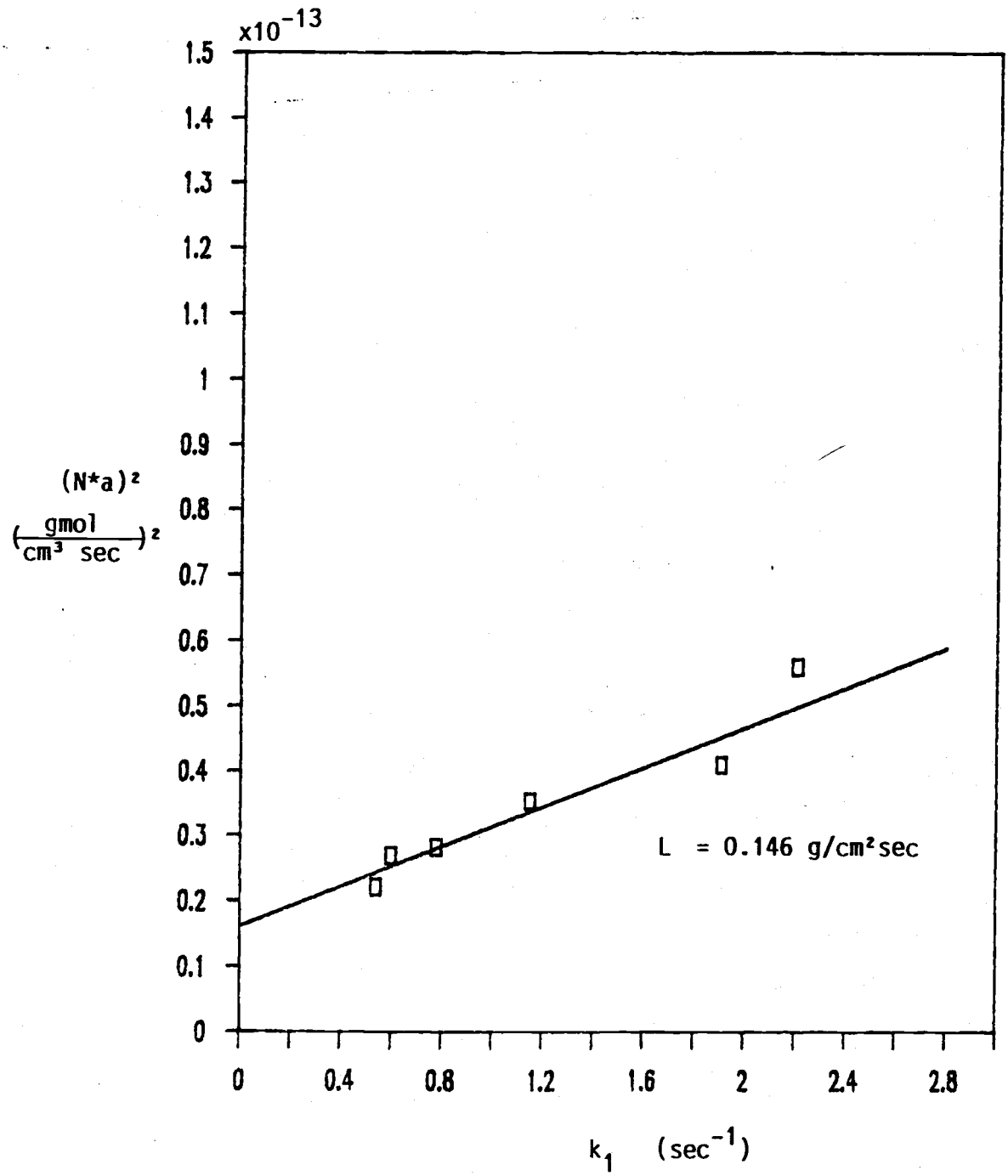

Figure 4 . Danckwerts type plot of $(N*a)^2$ and k_1 for ½-inch Raschig ring

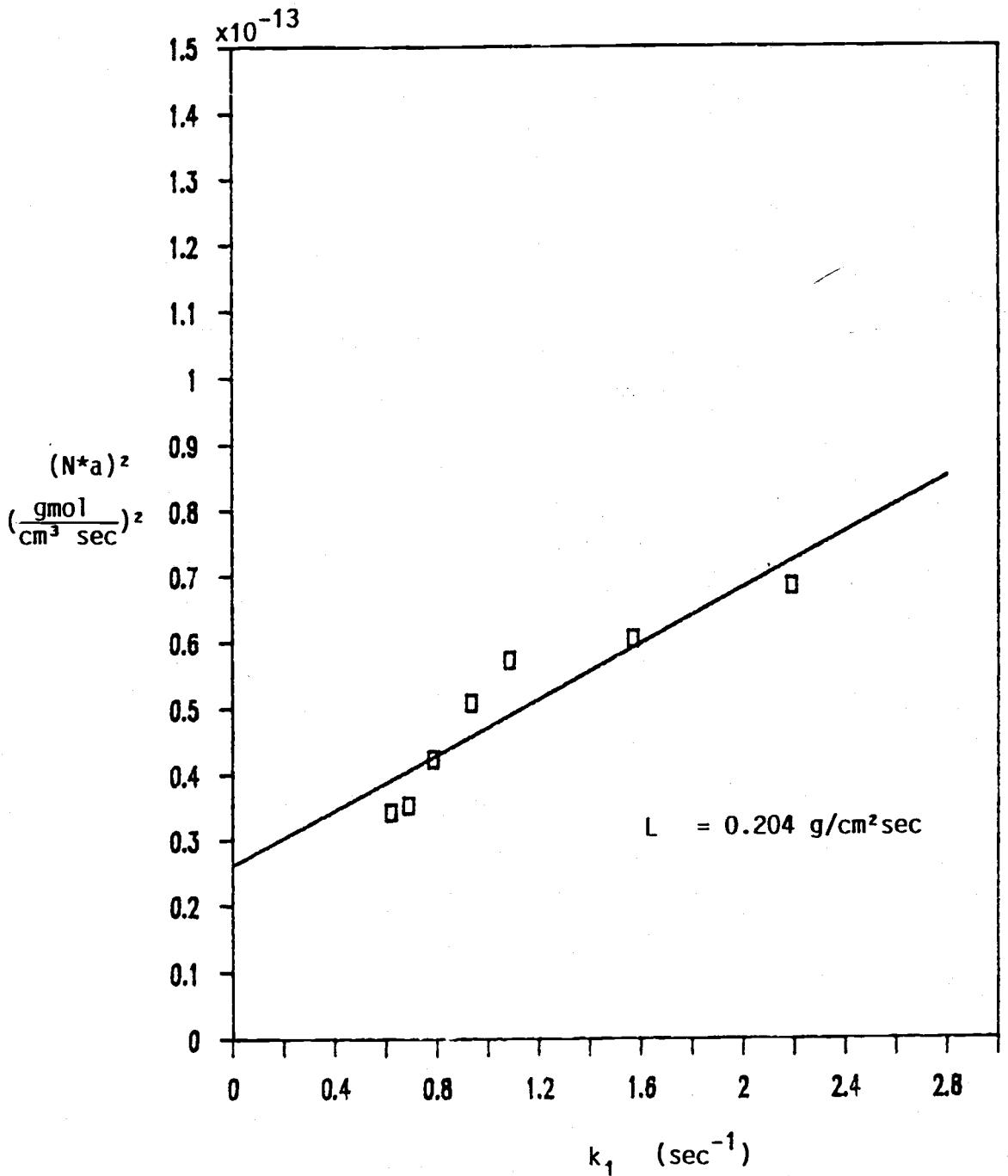

Figure 5 . Danckwerts type plot of $(N*a)^2$ and k_1 for ½-inch Raschig ring

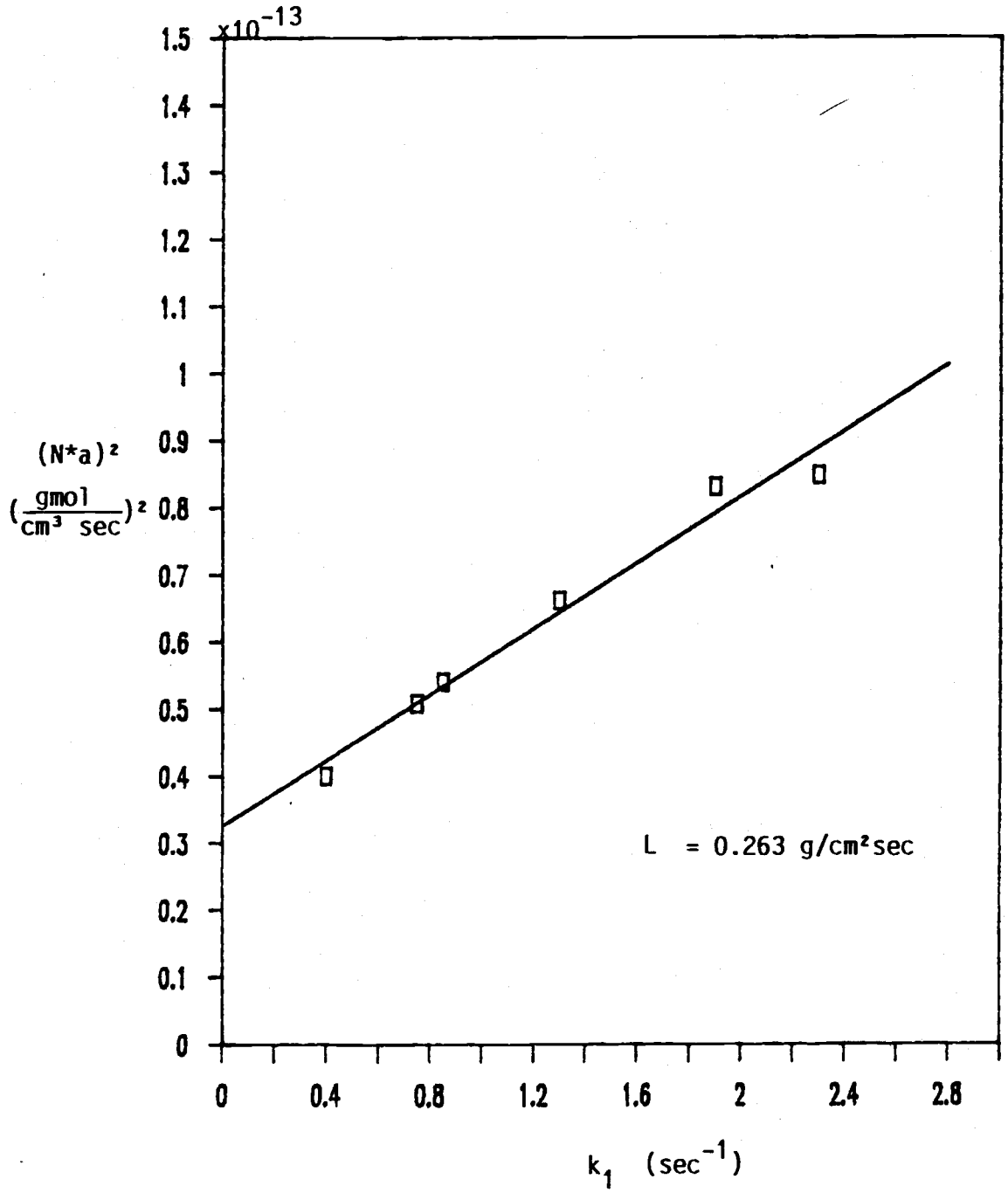

Figure 6 . Danckwerts type plot of $(N*a)^2$ and k_1 for ½-inch Raschig ring

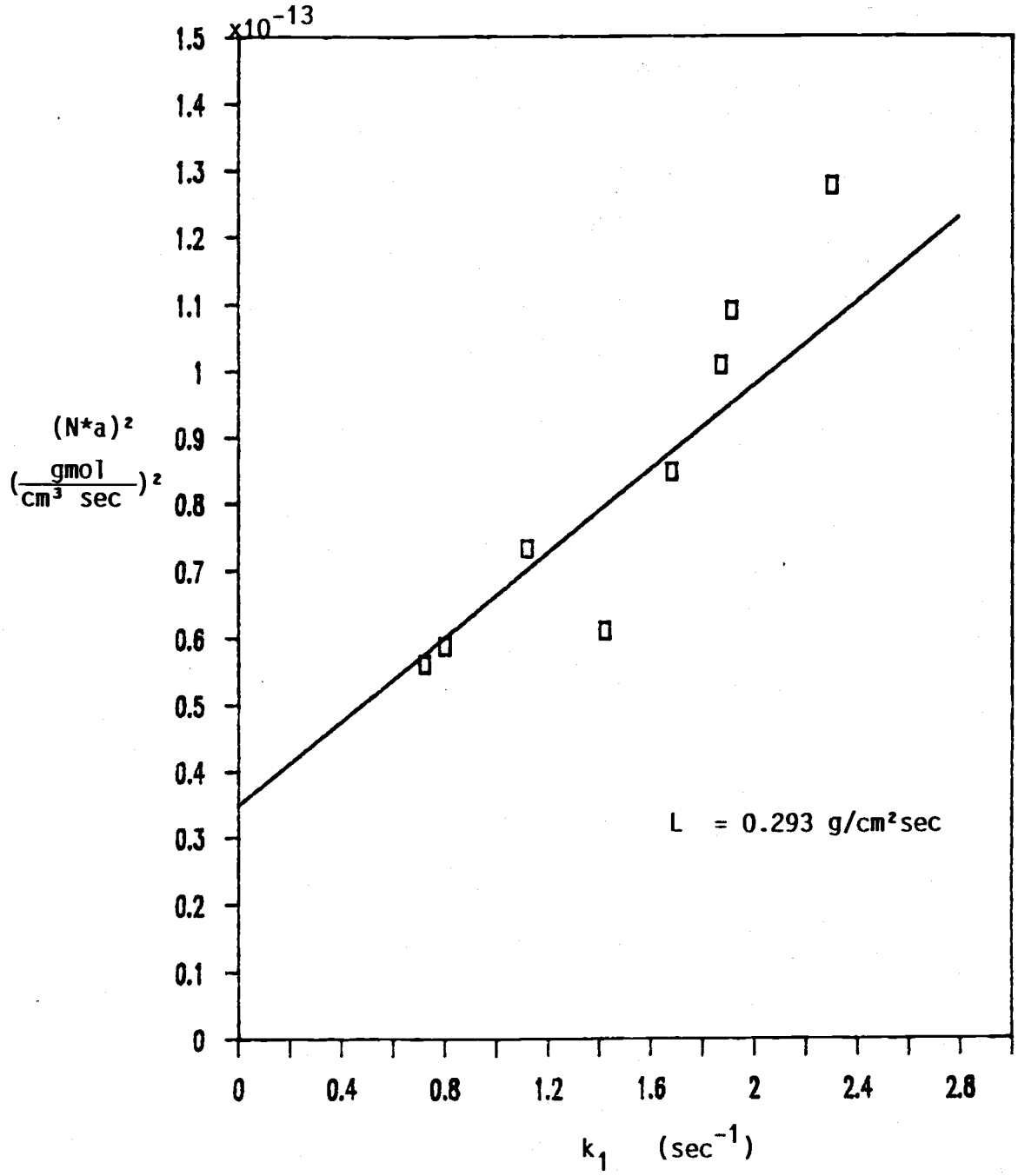

Figure 7 . Danckwerts type plot of $(N*a)^2$ and k_1 for ½-inch Raschig ring

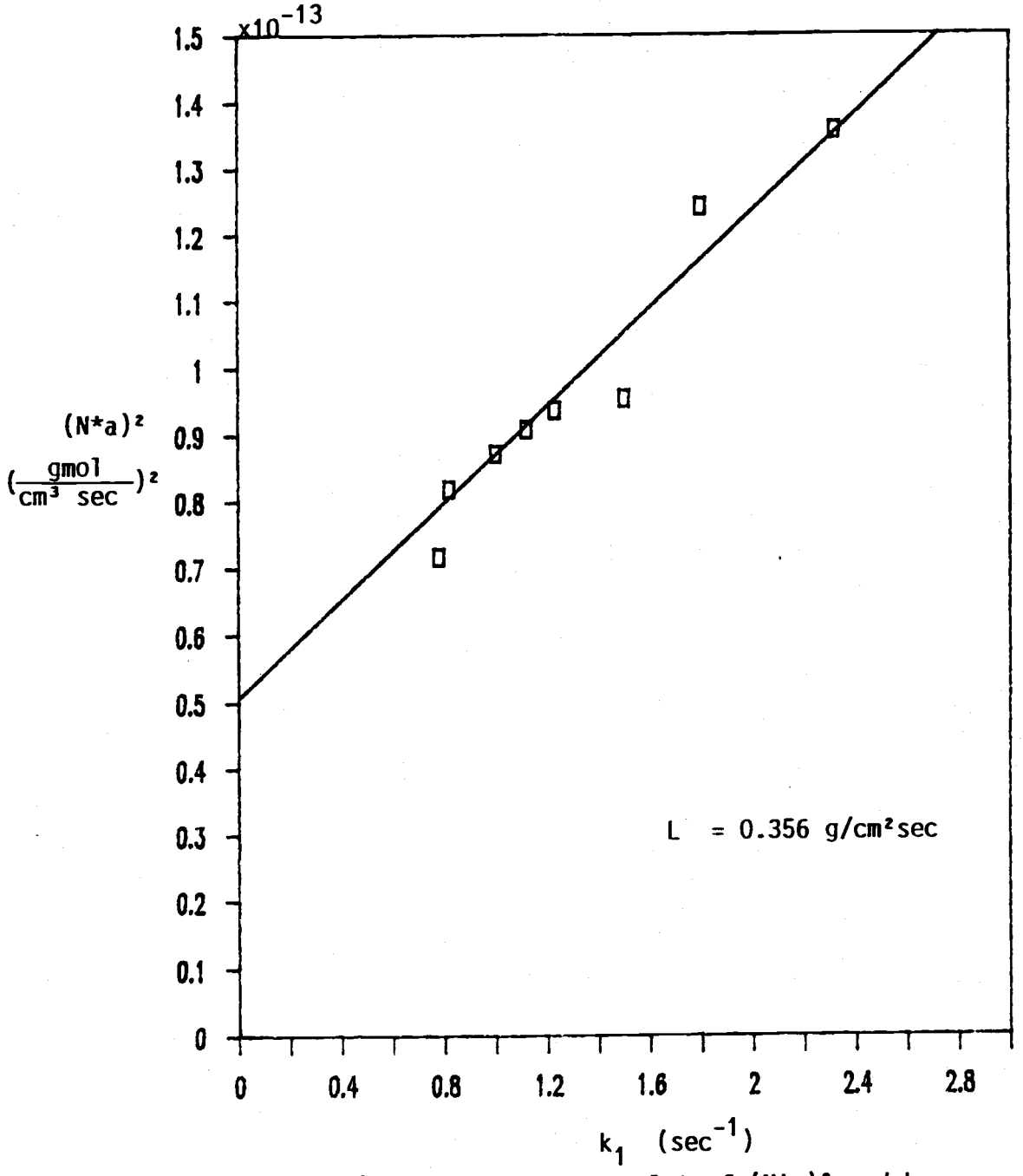

Figure 8. Danckwerts type plot of $(N*a)^2$ and k_1 for ½-inch Raschig ring

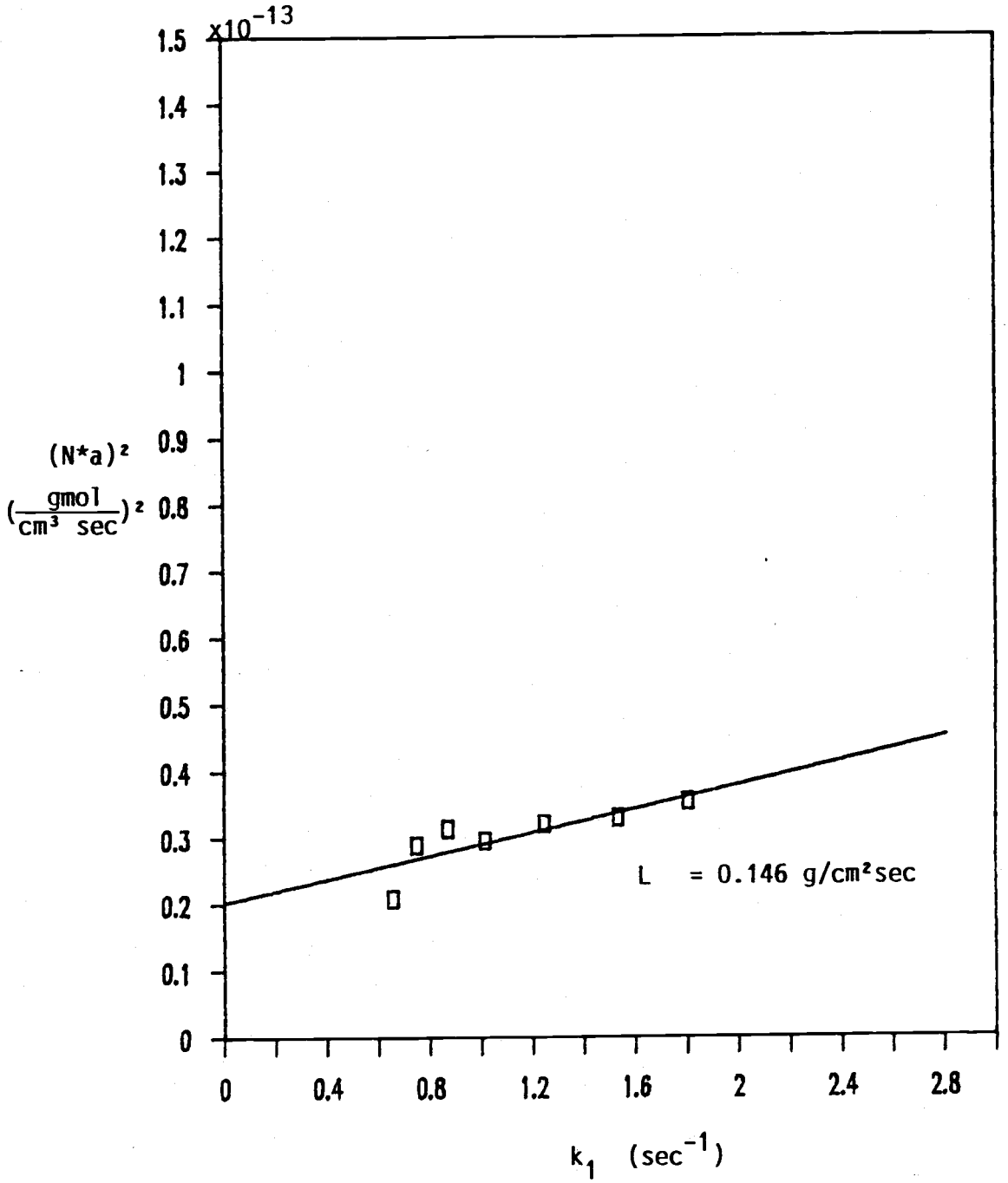

Figure 9 . Danckwerts type plot of $(N*a)^2$ and k_1 for ½-inch Berl saddle

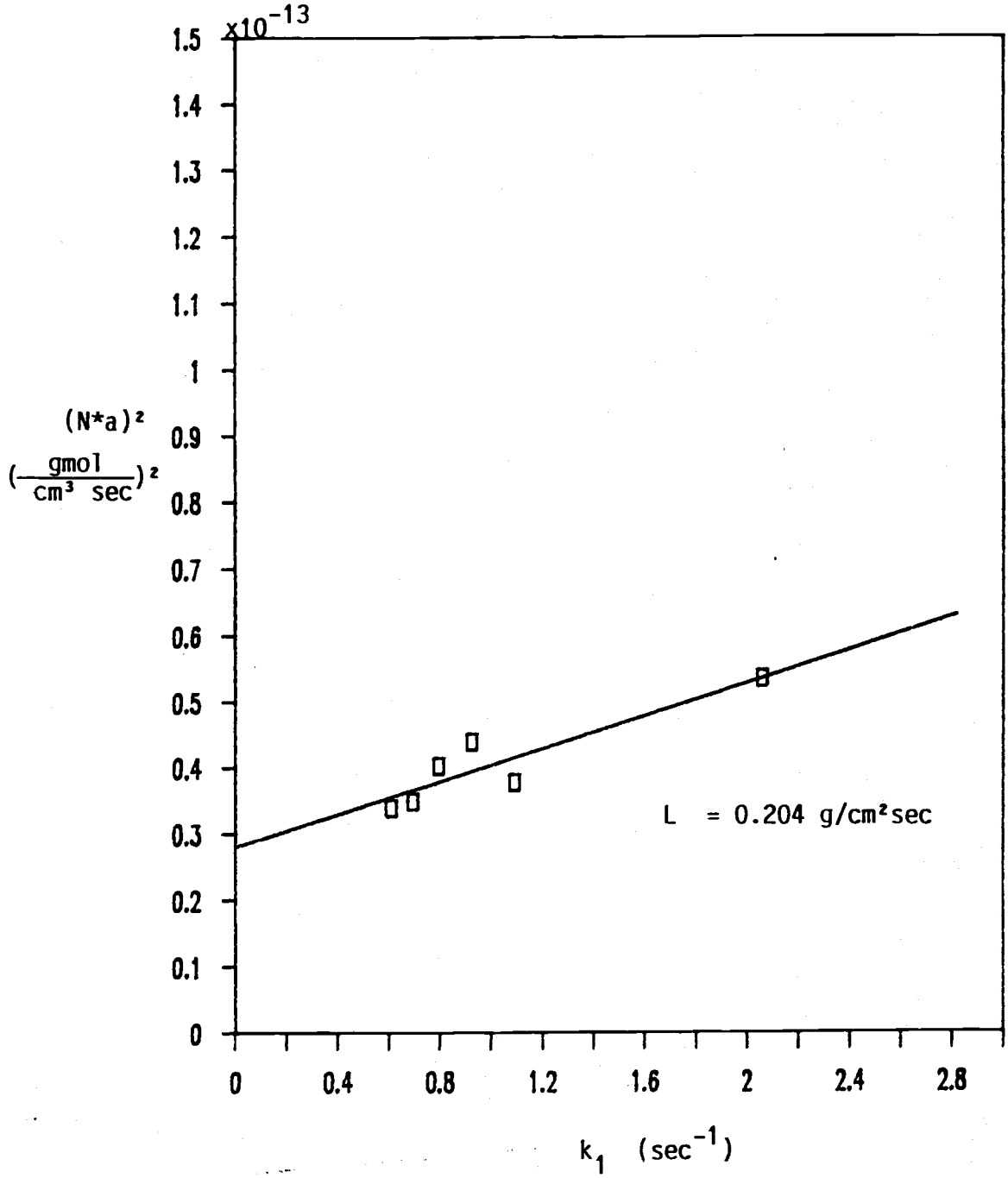

Figure 10 . Danckwerts type plot of $(N*a)^2$ and k_1 for ½-inch Berl saddle

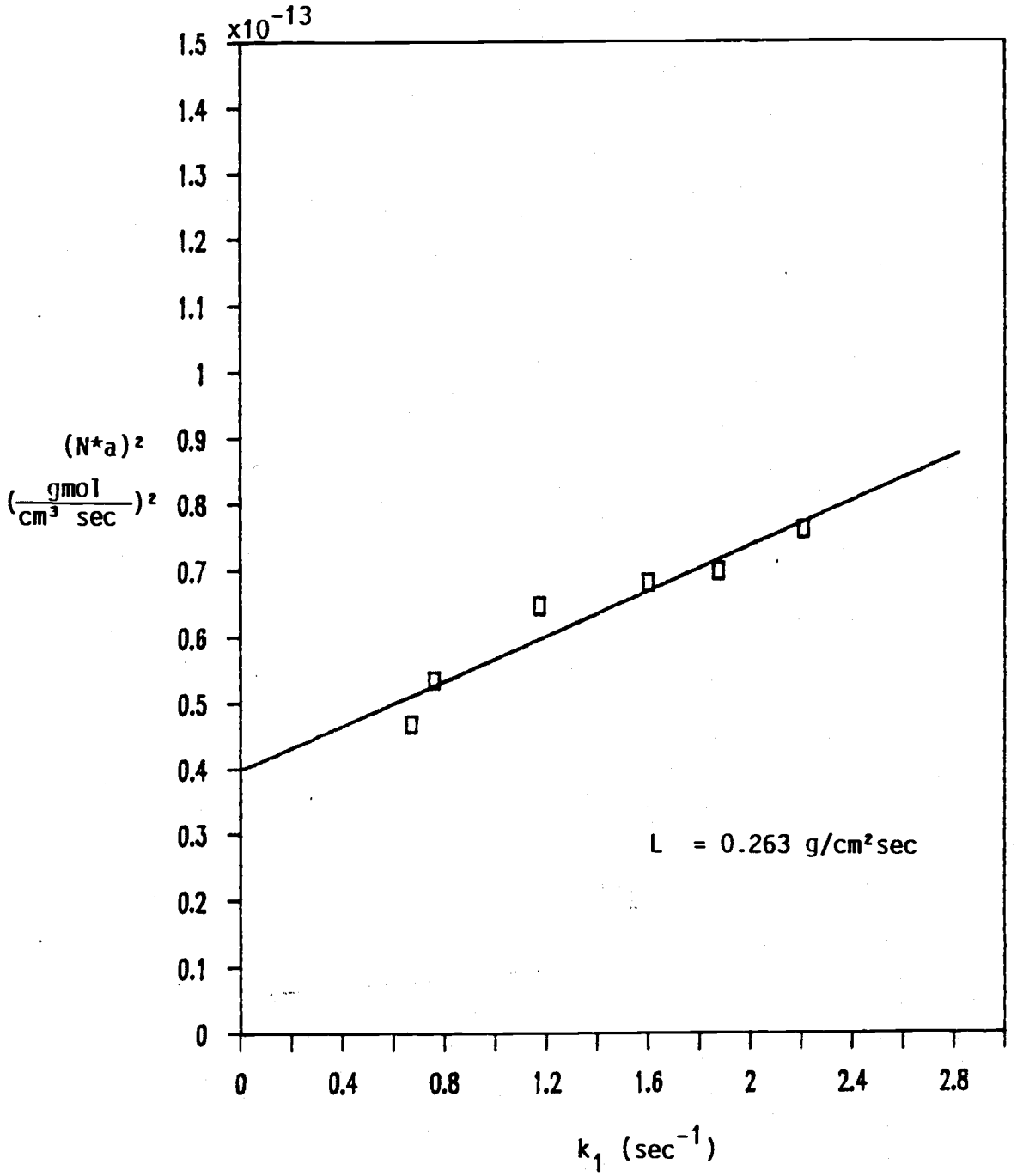

Figure 11 . Danckwerts type plot of $(N^*a)^2$ and k_1 for ½-inch Berl saddle

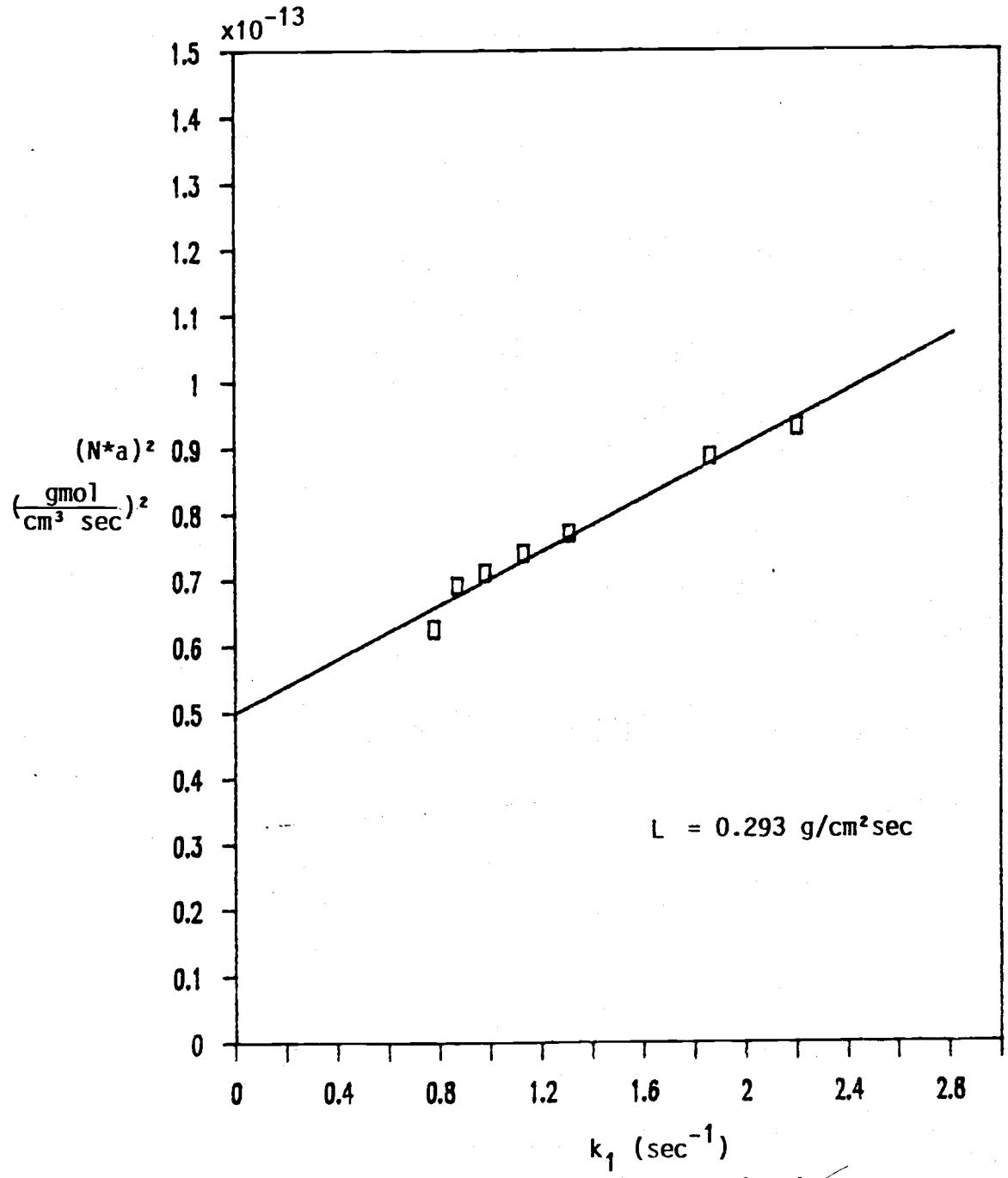

Figure 12. Danckwerts type plot of $(N*a)^2$ and k_1 for ½-inch Berl saddle

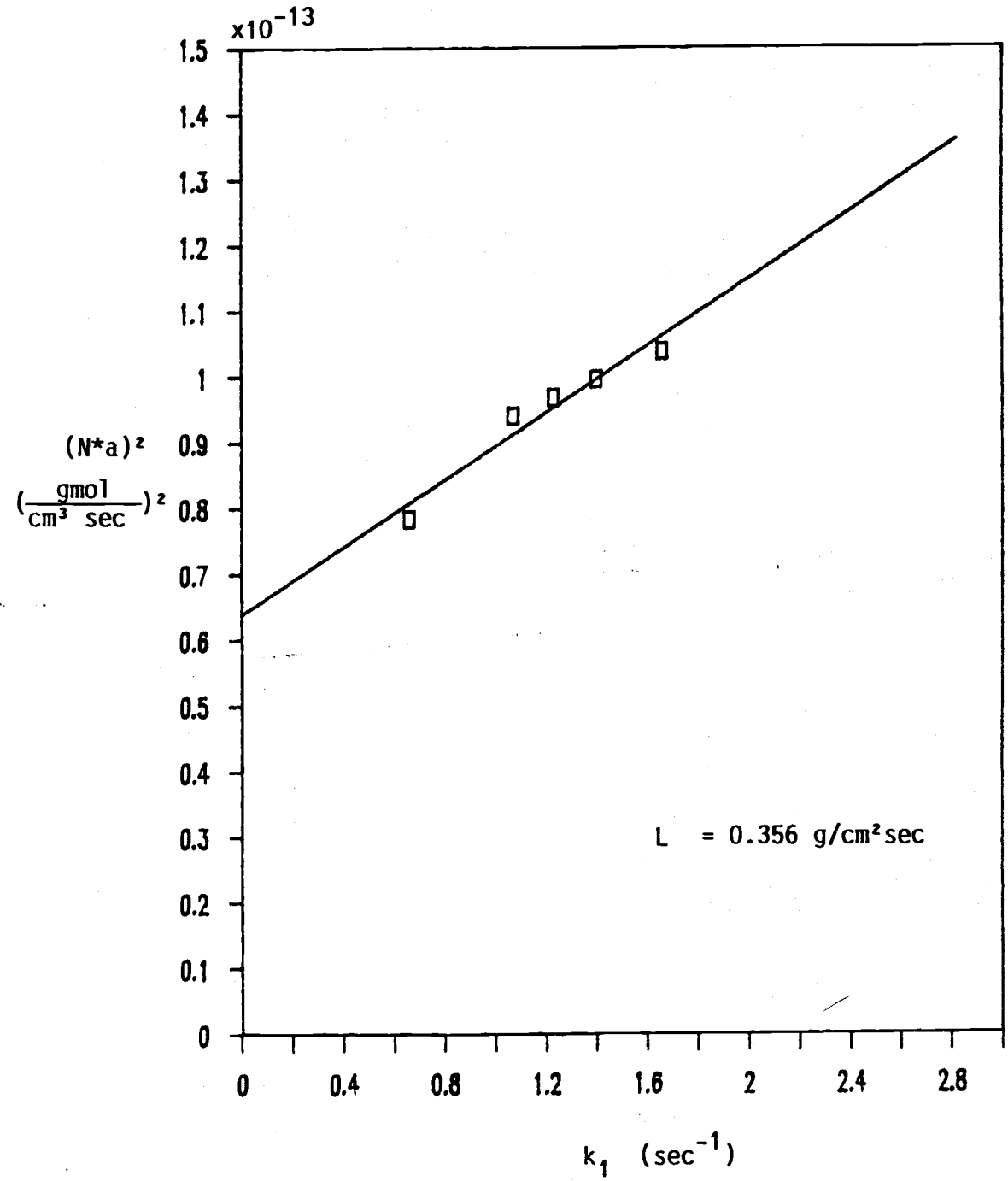

Figure 13. Danckwerts type plot of $(N*a)^2$ and k_1 for ½-inch Berl saddle

$$\log \frac{c^*}{c_w^*} = -k_s I \qquad (49)$$

where c_w^* is the saturation concentration in water at the given temperature[23]. At 25°C, c_w^* is equal to $3.28*10^{-2}$ gmol/liter[26]. In the right side of equation, I is the ionic strength of the solution which can be calculated as $I = \frac{1}{2} \sum c_i z_i^2$ and k_s is the salting-out parameter. From Nysing and Kramer[25], k_s was equal to 0.088 for sodium buffer solution. The mass diffusivity, D, of CO_2 in sodium buffer solution was obtained from Hikita's equation[26]

$$\frac{D}{D_w} = 1 - (\S_1 c_1 + \S_2 c_2 + \S_3 c_3) \qquad (50)$$

where $\S_1$ is equal to 0.261 for Na_2CO^3, $\S_2$, 0.140 for $NaHCO_3$ and $\S_3$, 0.129 for NaOH. D_w is the mass diffusivity in water at a given temperature and c_i is the concentration of each component. D_w used here was $1.92*10^{-5}$ cm_3/sec from Hikita[26]. The values of c^* and D for this experiment were equal to $2.03*10^{-5}$ gmol/cm^3 and $1.486*10^{-5}$ cm^2/sec. Therefore, $c^*\sqrt{D}$ was $7,85*10^{-8}$gmol/$cm^2 sec^{\frac{1}{2}}$ in equation(22).

The values of s and a are given on each plot and are summarized in Table I and Table II. Upon inspection of the tables, one can observe that the value of the surface renewal rate, s, increases with liquid flow rates. Figure 14 and 16 illustrate the surface renewal rate dependence on Reynolds number. Earlier investigators have presumed that the surface renewal rate was probably a function of the Reynolds number as expressed

$$s = \tilde{a}\, Re^n \qquad (51)$$

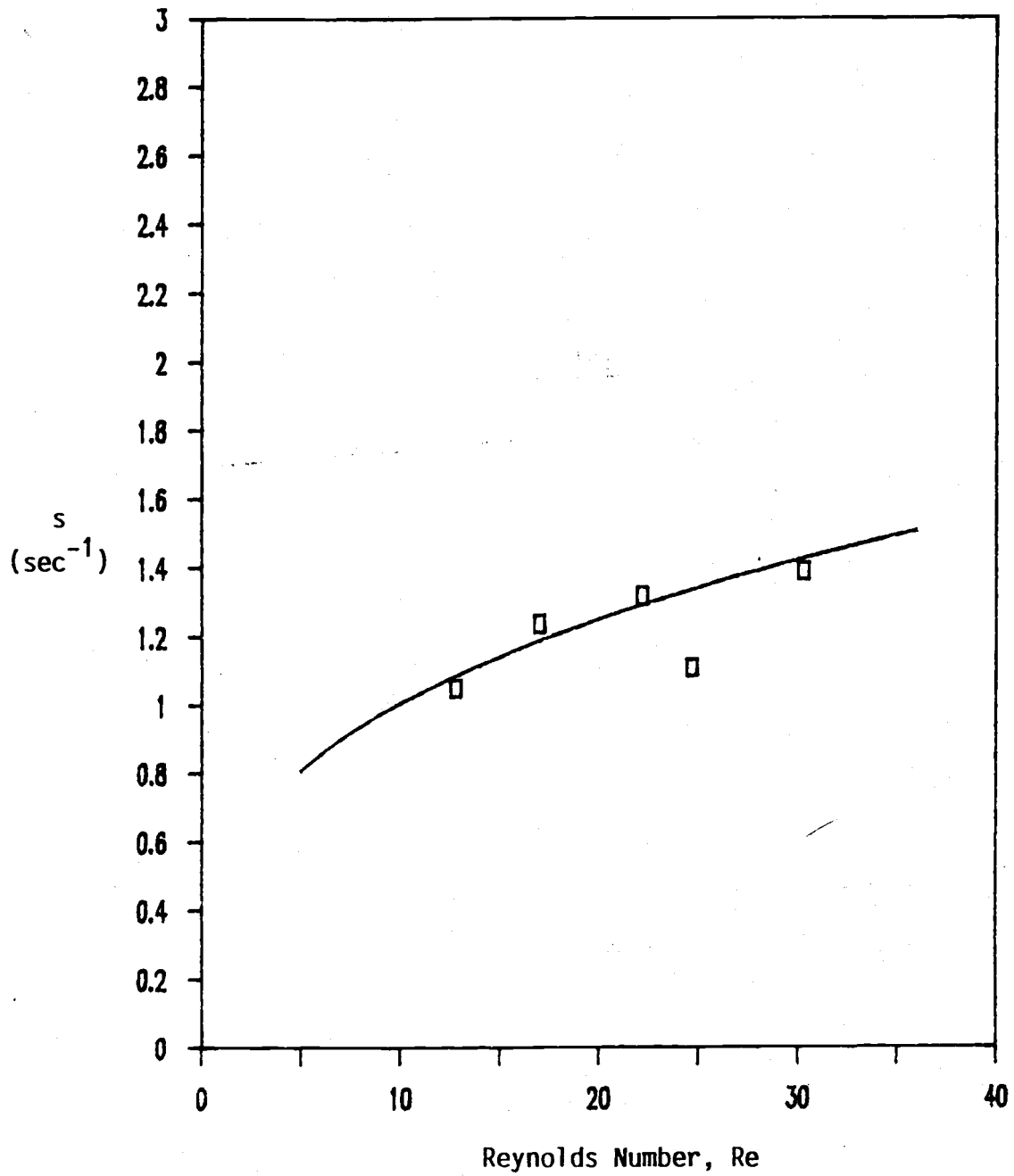

Figure 14. Reynolds number and s for Raschig ring

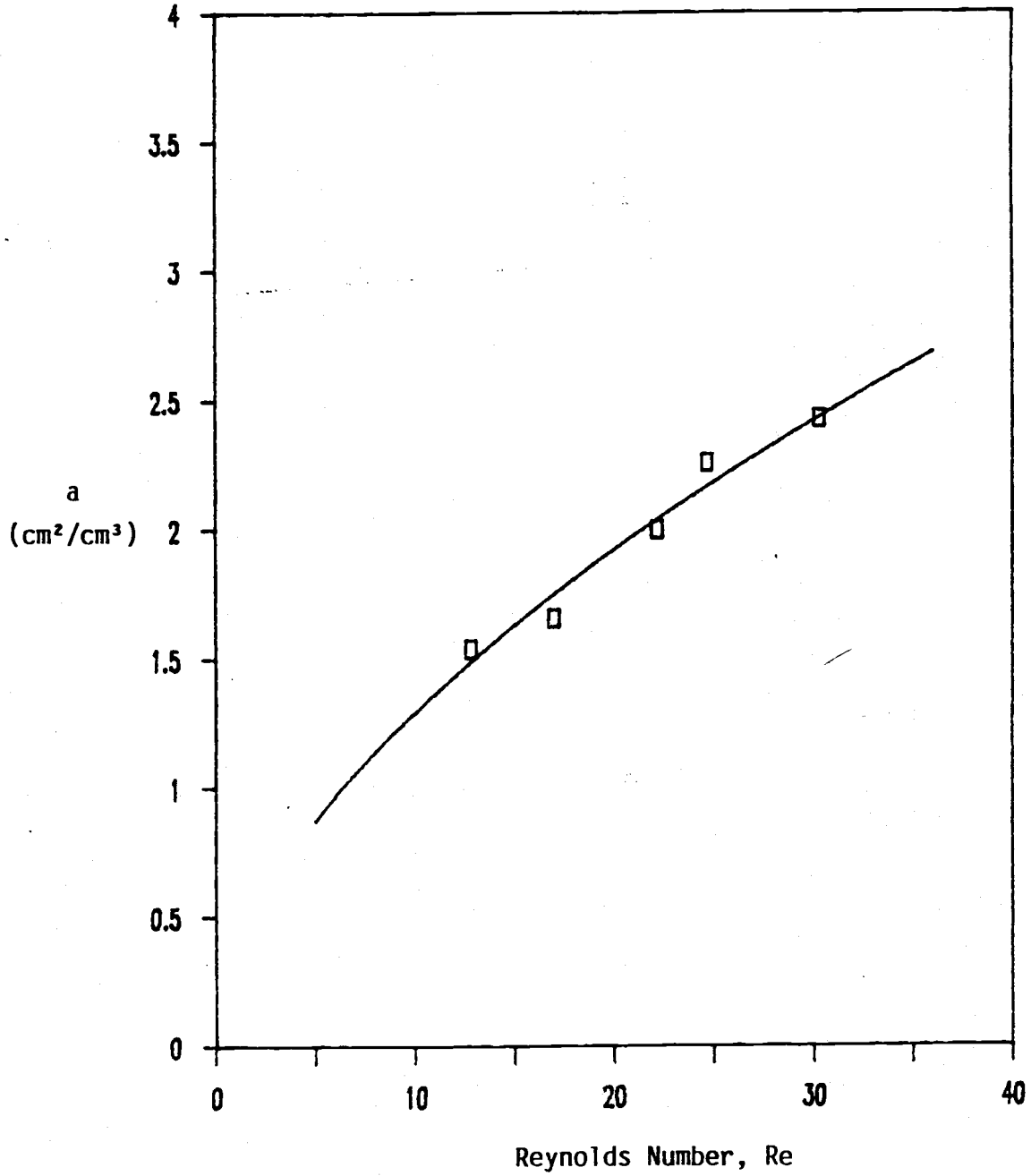

Figure 15. Reynolds number and a for Raschig ring

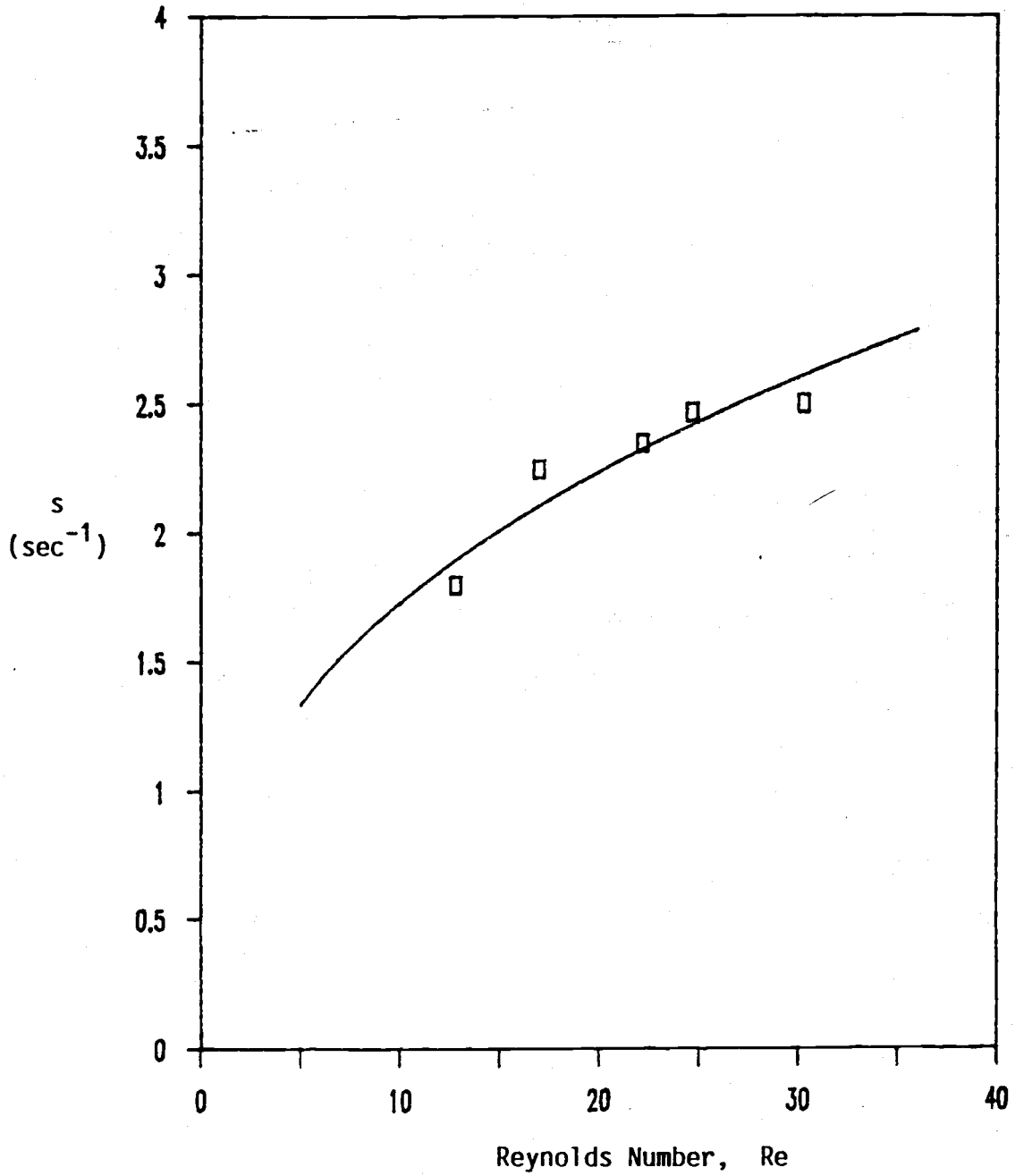

Figure 16. Reynolds number and s for Berl saddle

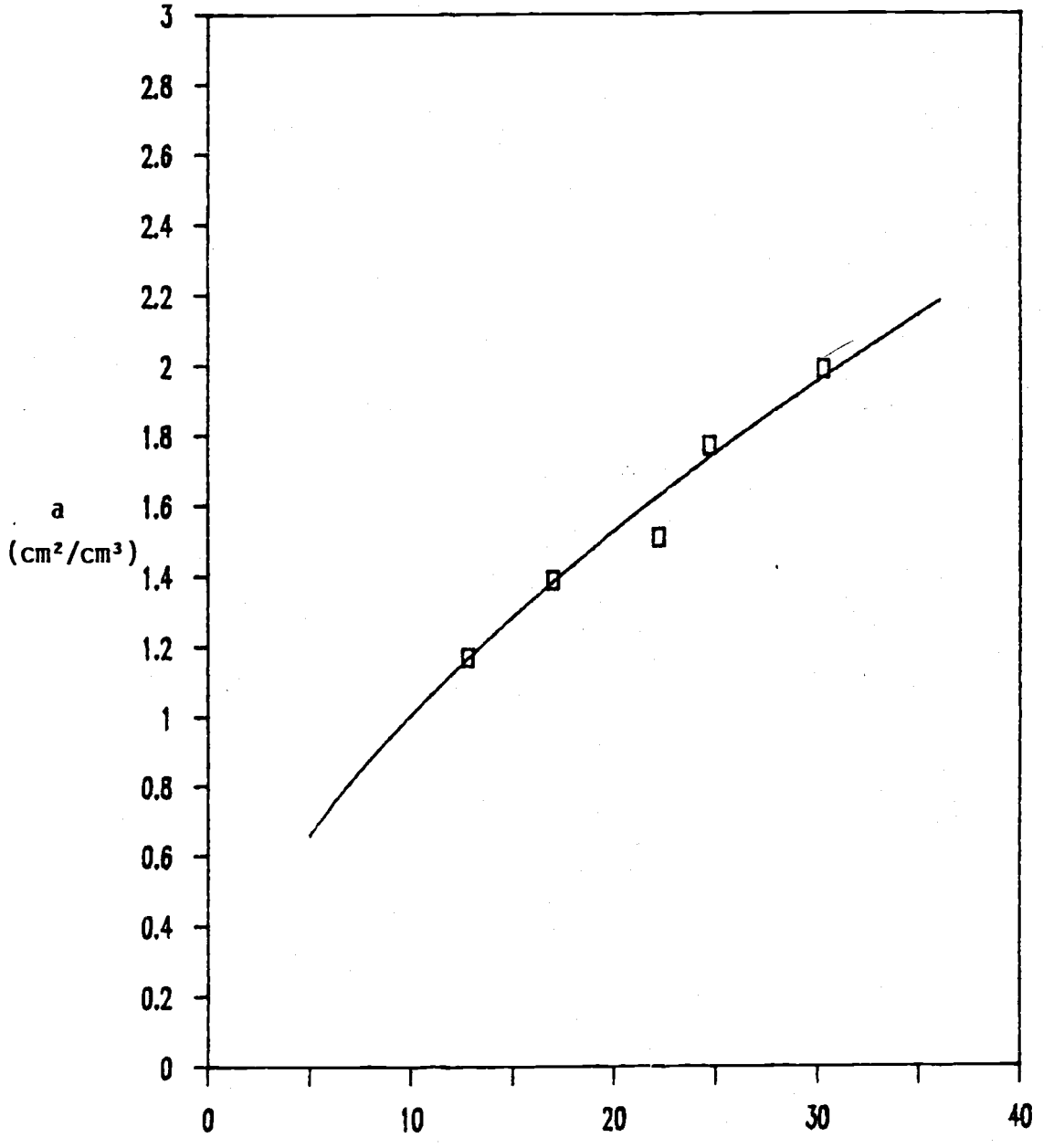

Figure 17. Reynolds number and a for Berl saddle

Table I. Surface renewal rate and effective interfacial area for ½-inch Raschig ring with 300 cm^3/sec gas flow rate

Liquid flow rate(g/cm^2sec)	$s(sec^{-1})$	$a\ (cm^2/cm^3)$
0.146	1.05	1.54
0.204	1.24	1.66
0.263	1.32	2.00
0.293	1.11	2.26
0.356	1.39	2.43

Table II. Surface renewal rate and effective interfacial area for ½-inch Berl saddle with 300 cm^3/sec gas flow rate

Liquid flow rate(g/cm^2sec)	$s(sec^{-1})$	$a(cm^2/cm^3)$
0.146	1.80	1.17
0.204	2.25	1.39
0.263	2.35	1.51
0.293	2.47	1.77
0.356	2.50	1.99

where the Reynolds number is defined at the following ratio of physical properties and physical variables of liquid

$$Re = \frac{(\text{packing piece diameter})(\text{velocity})(\text{density})}{(\text{viscosity})}$$

This equation should plot a straight line when the data are plotted as log s versus log Re. Figure 18 presents this plot for the ½-inch Raschig ring with ã equal to 0.49 and n equal to 0.32 and another straight line for ½-inch Berl saddle with ã=0.74 and n equal to 0.37. The same method was used to obtain the relationship between the effective interfacial area, a, and Re in Figure 19 for $a = ß\ Re^m$. From this figure, ß is 0.35, m equal to 0.57 for ½-inch Raschig ring and ß equal to 0.25 and m equal to 0.61 for ½-inch Berl saddle.

In the experimental studies involving absorption accompanied by first-order reaction, the tower diameter and the density and viscosity of the solutions were essentially constant. Accordingly, the equation obtained

$$s = ã\ Re^n \tag{51}$$

really shows how the surface renewal rate is a function of the liquid flow rate

$$s = ã'\ (L')^n \tag{52}$$

In an effort to determine whether the other variables affect the mass transfer, changes of in the viscosity and the density of the solution were considered. It was decided to use a glycerine-water solution; the viscosity and the density of this solution could be varied easily by changing

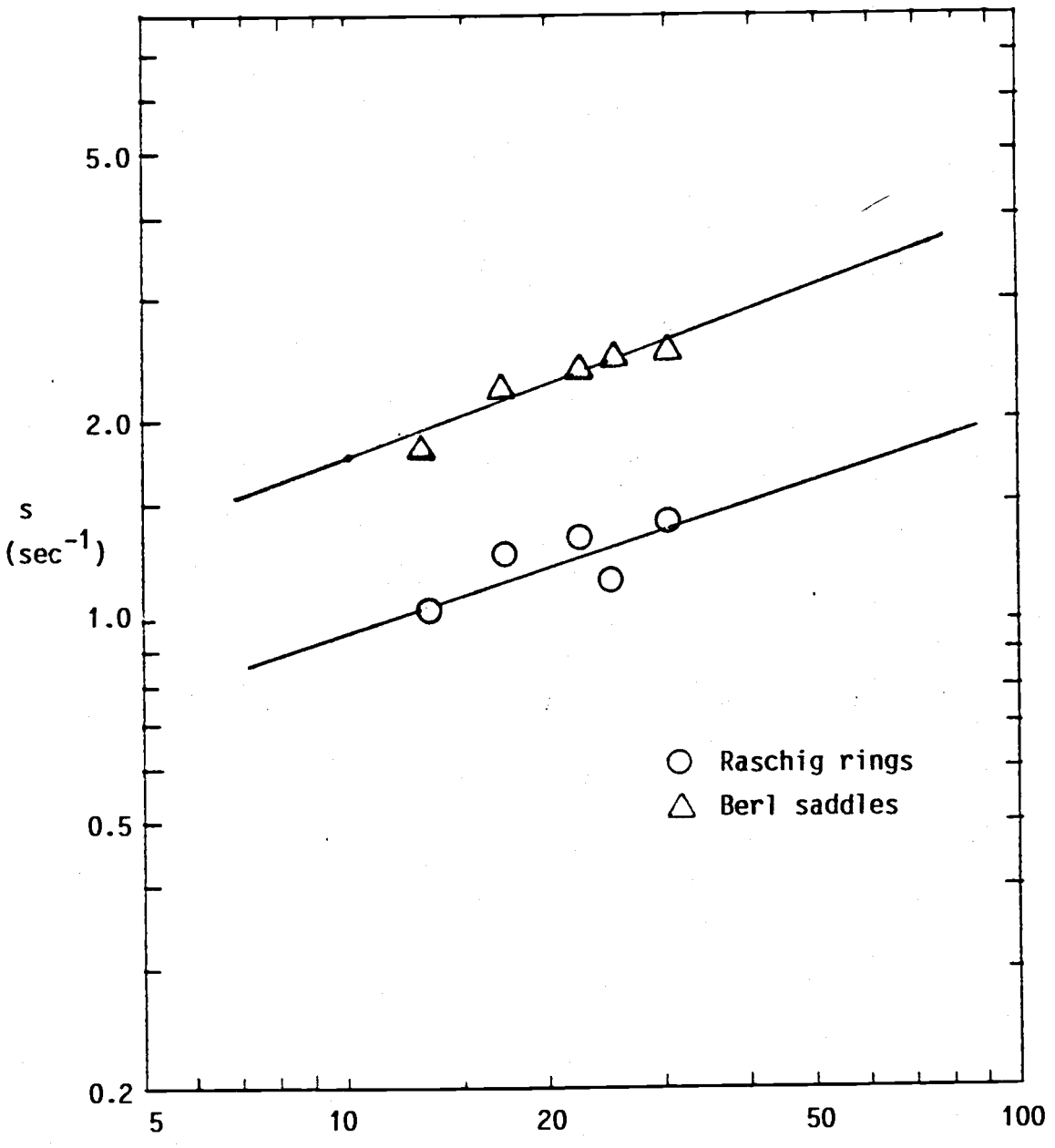

Figure 18. Log Re and Log s

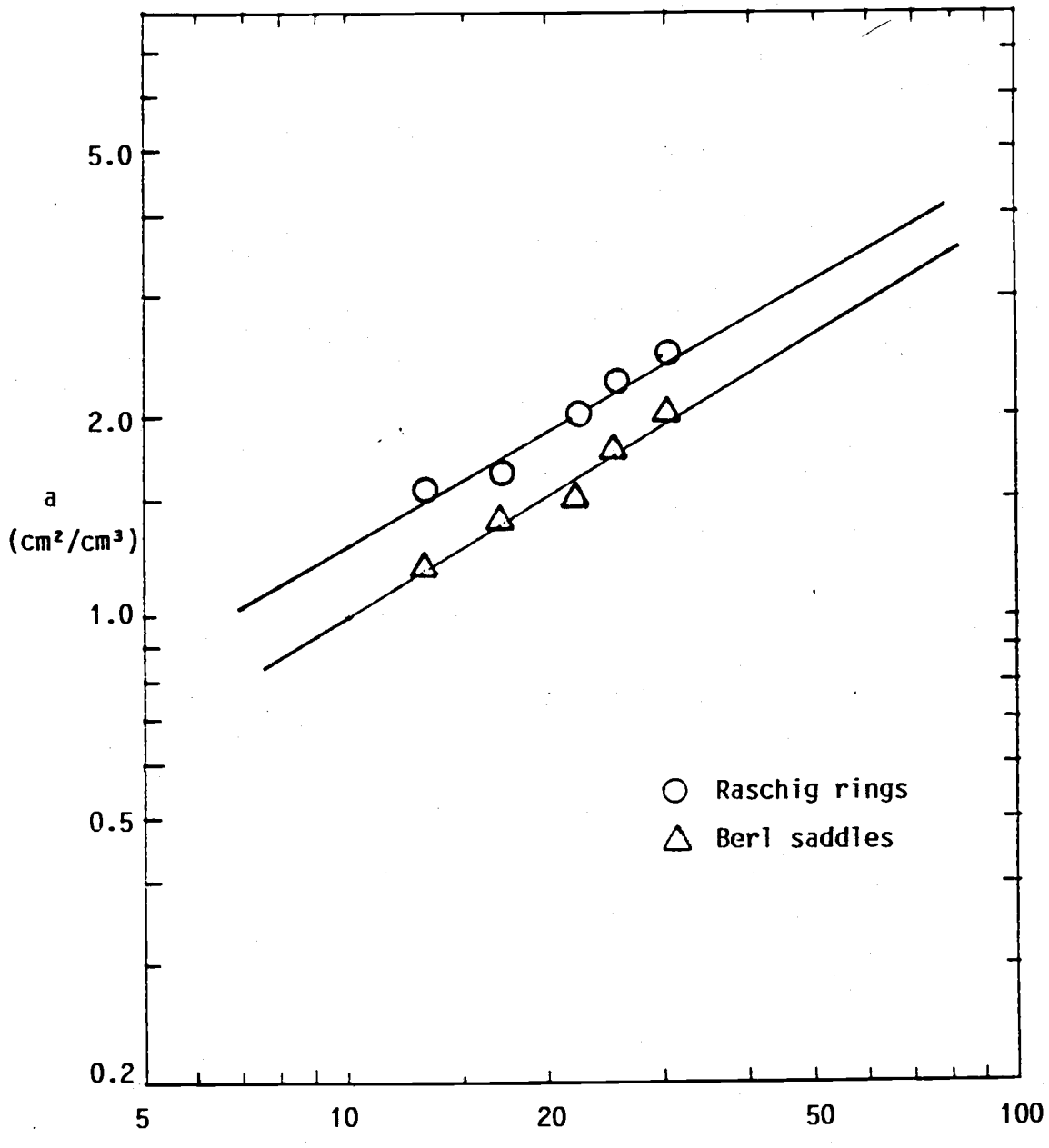

Figure 19. Log Re and Log a

the content of glycerine in the solution. The physical properties of the solution, including the mass diffusivity and the saturated concentration of CO_2 in the solution, have been obtained by previous researcher[27]; these values are plotted in Appendix II. Unfortunately, data were not available for chemical kinetics inside the glycerine-carbonate/bicarbonate buffer solution. Accordingly, only mass transfer by physical absorption into the pure water and into aqueous solutions of varying concentration of glycerine were studied.

Mass transfer coefficients per unit volume of packed section versus Reynolds number were plotted in Figure 20 through 24 for solutions containing different amount of glycerine.

To obtain the relationships of mass transfer coefficients with Reynolds number, $\log(k_L*a/D)$ versus log Re were plotted for different viscosities of solutions in Figure 25. From these plots, an equation, $k_L*a/D = \gamma*Re^P$ was determined which related k_L*a/D to the Reynolds number; the exponent p was found to be a constant 0.72, and the coefficient γ was found to depend on the Schmidt number, Sc or $(\mu/\rho D)$. In Figure 26, the plot of log versus log Sc gave the relationship as $\gamma = 1.55\ Sc^{0.5}$. Accordingly, the mass transfer coefficient for absorption without chemical reaction is as follows

$$\frac{k_L*a}{D} = 1.55\ Re^{.72}\ Sc^{.5} \qquad \begin{matrix} 20 \leq Re \leq 130 \\ 525 \leq Sc \leq 3390 \end{matrix} \qquad (53)$$

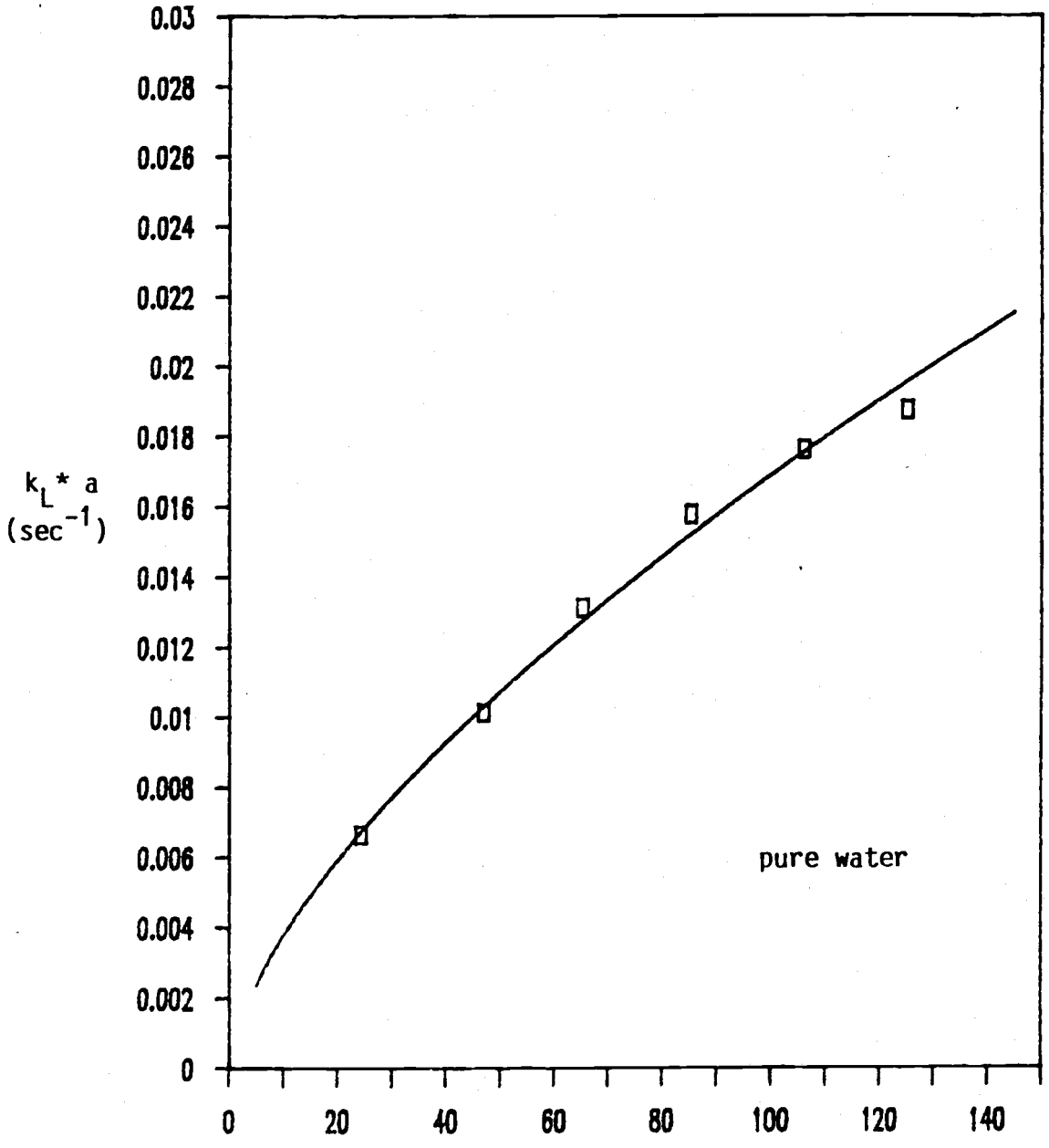

Figure 20. Reynolds number and mass transfer coefficient for water-glycerine solution

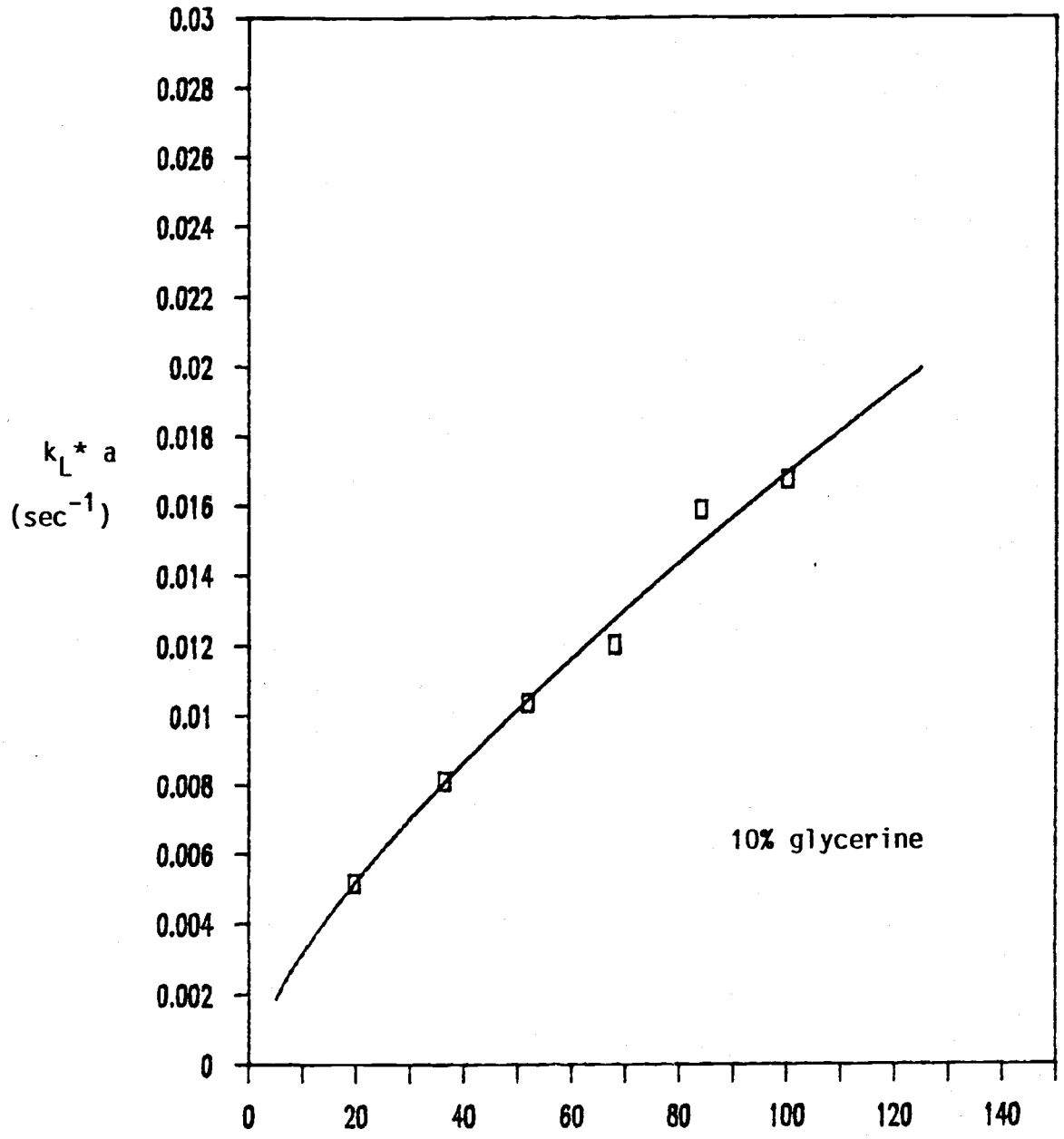

Figure 21. Reynolds number and mass transfer coefficient for water-glycerine solution

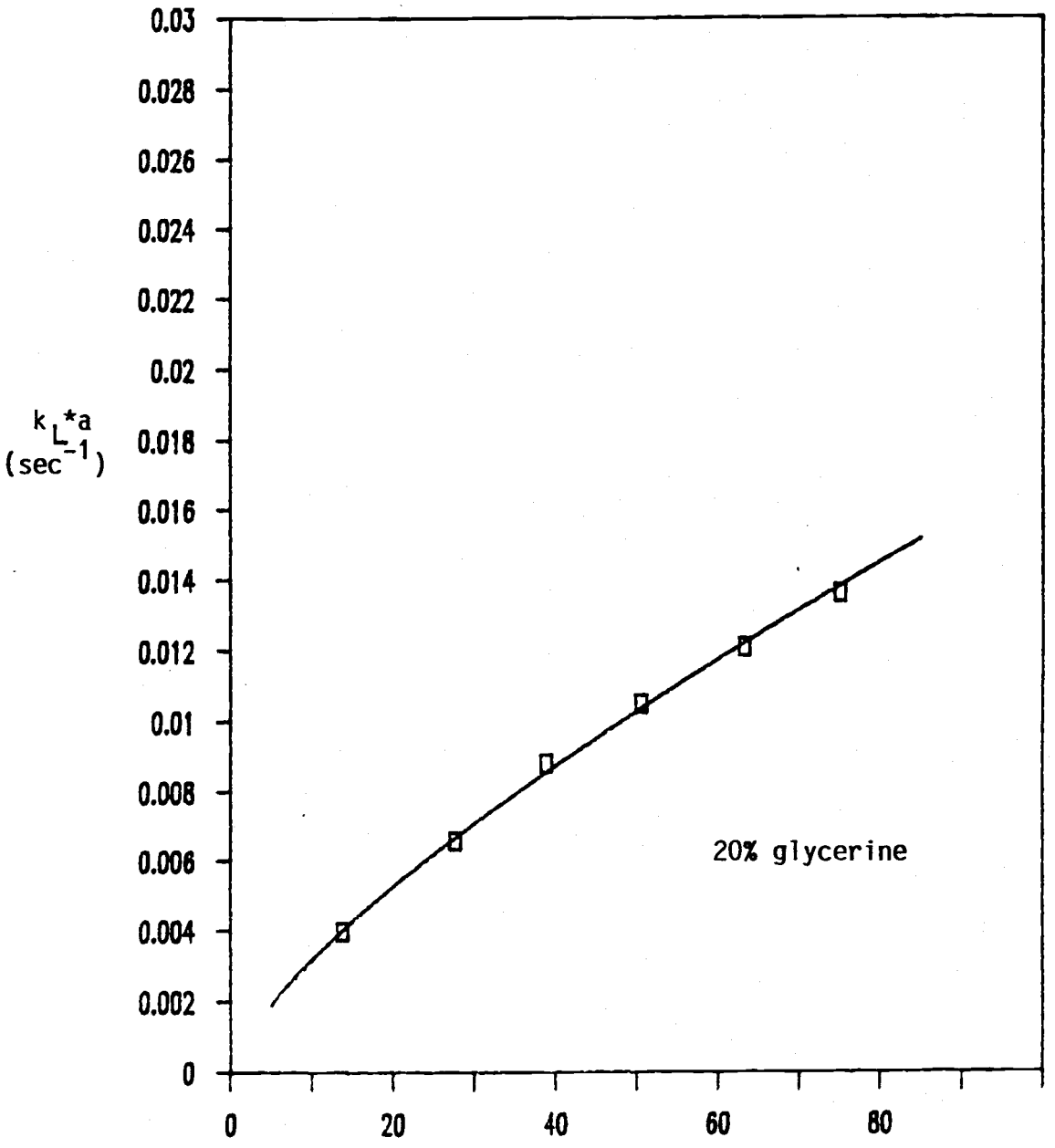

Figure 22. Reynolds number and mass transfer coefficient for water-glycerine solution

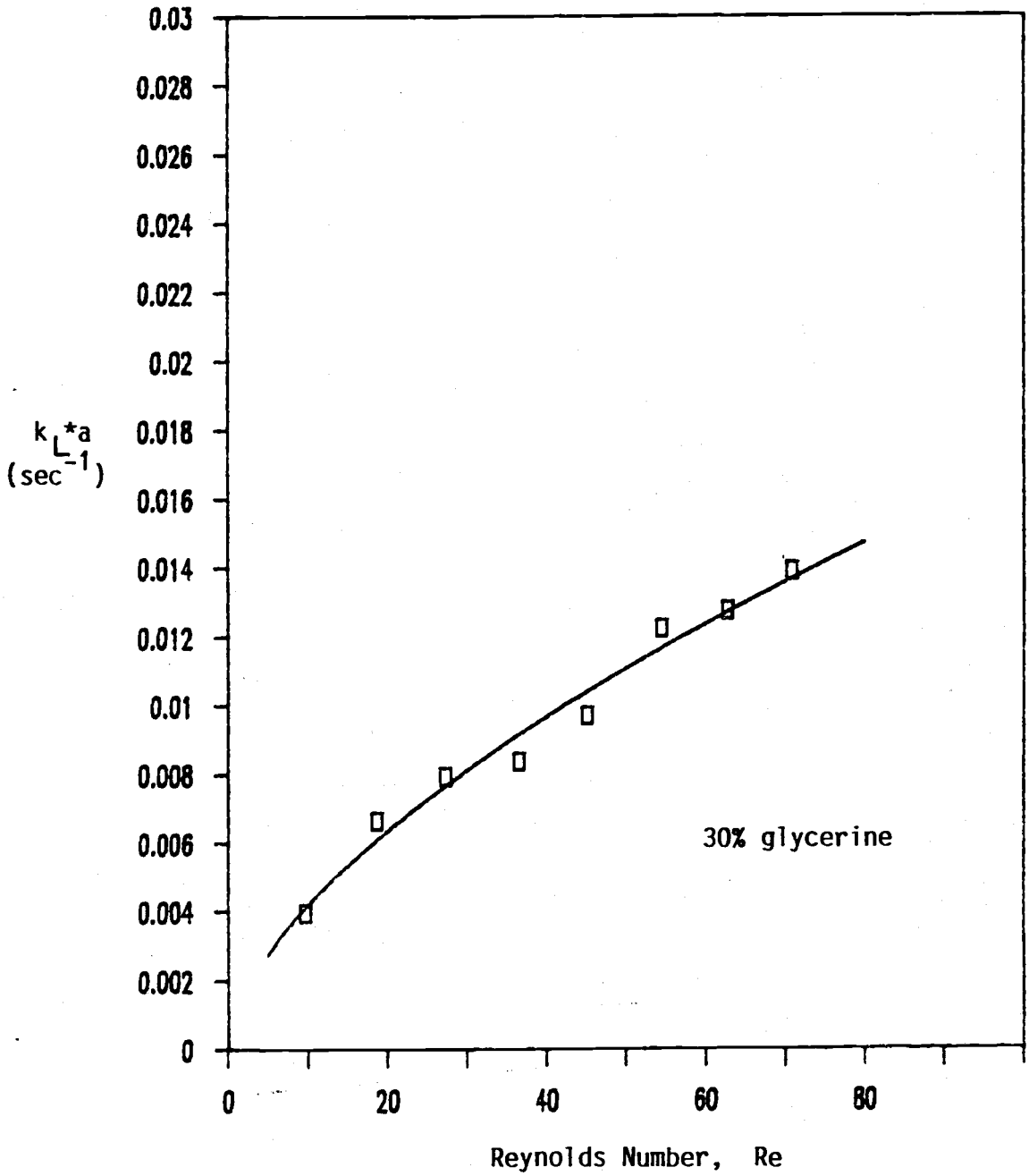

Figure 23. Reynolds number and mass transfer coefficient for water-glycerine solution

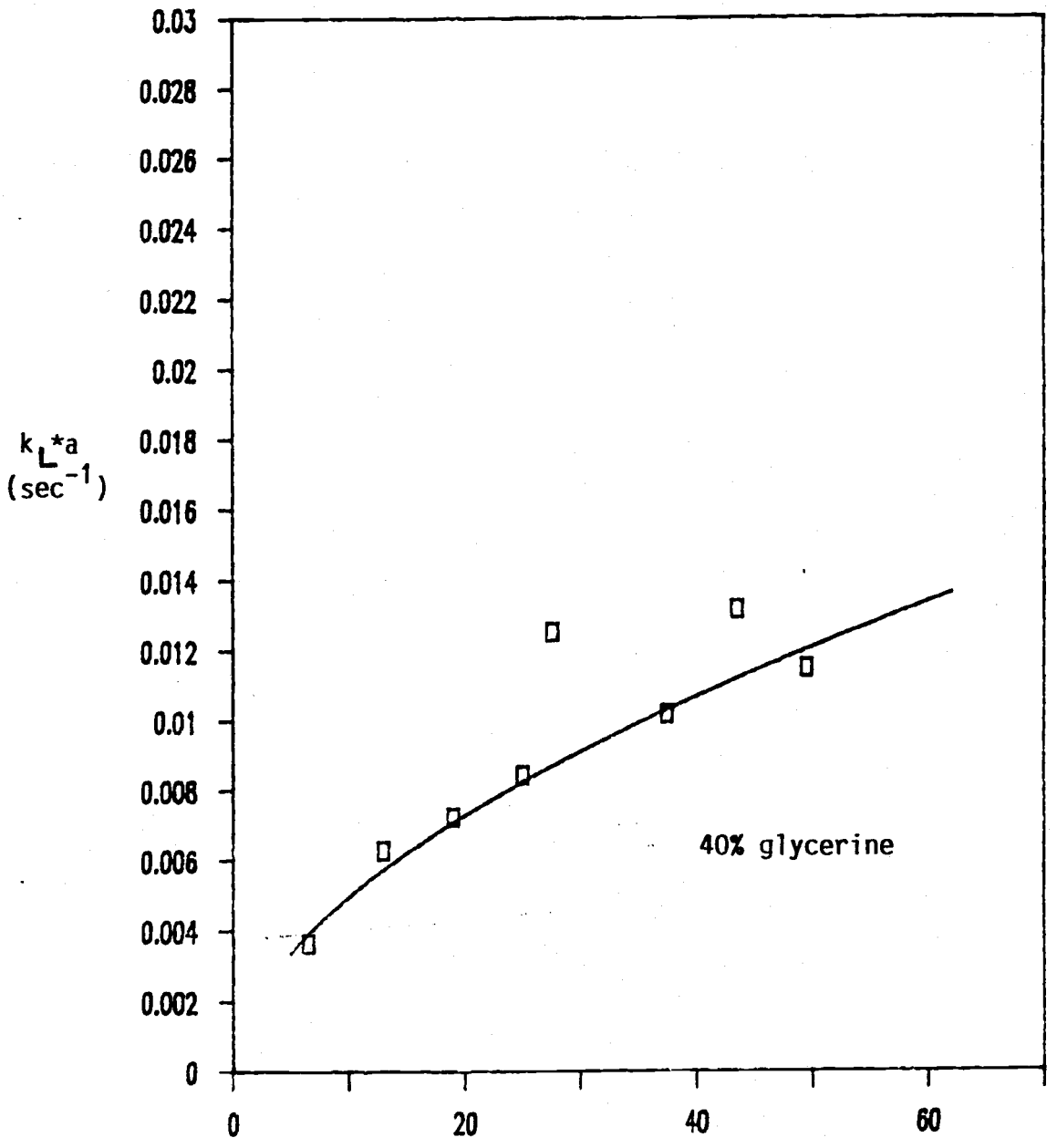

Figure 24. Reynolds number and mass transfer coefficient for water-glycerine solution

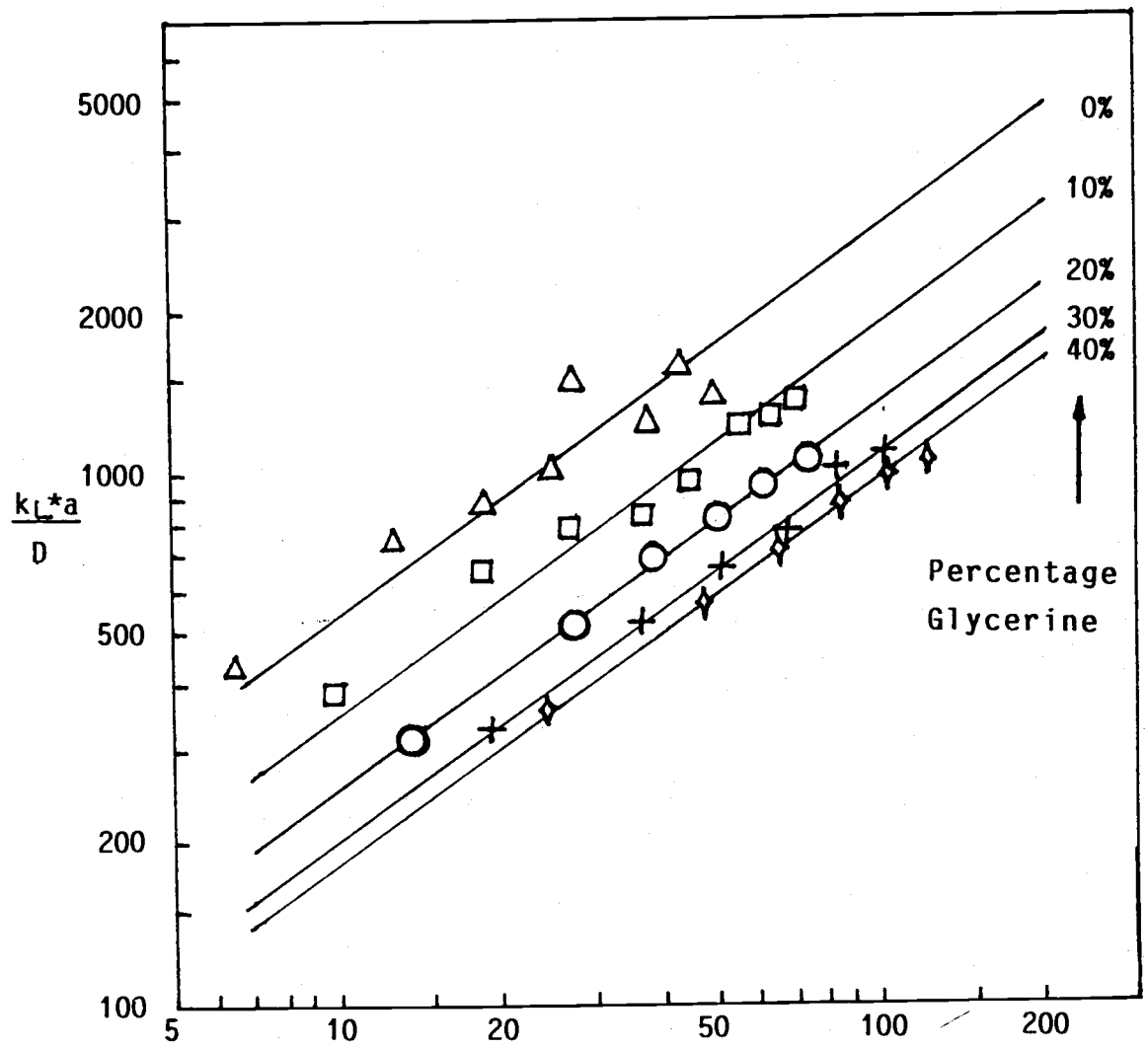

Figure 25. Log Re and Log $\frac{k_L * a}{D}$

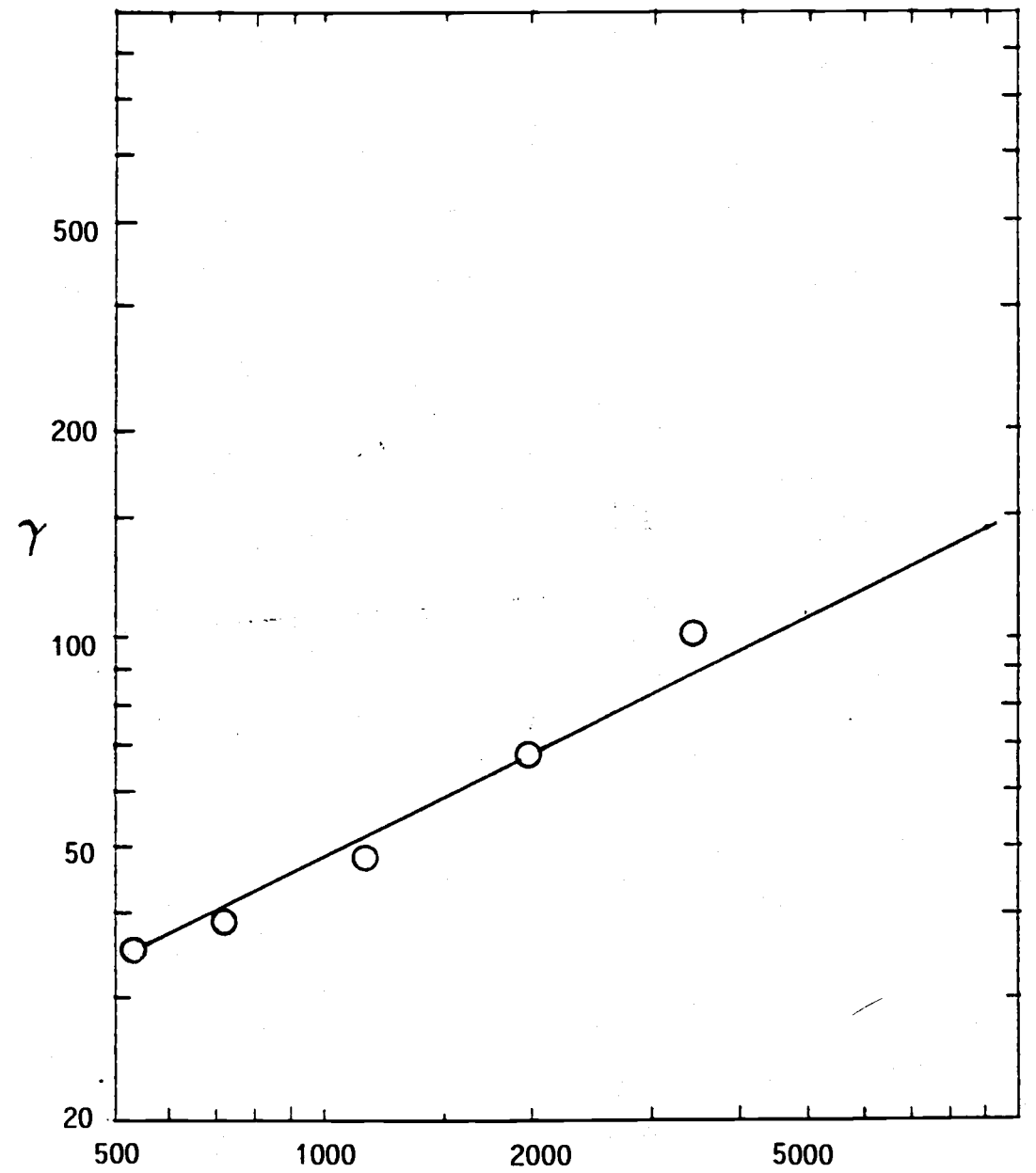

Figure 26. Log Sc and Log γ

Table III. γ values with Schmidt numbers of the solution

Sc	γ
525	35.1
720	39.1
1150	48.4
1970	67.5
3390	102.9

The equation shows that the mass transfer coefficient is proportional to the square root of diffusivity of solute in the solution, as predicted in Danckwerts' theory.

The summary of the results are as follows:

the surface renewal rates, s (sec^{-1})

$s = 0.49\ Re^{0.32}$ max. error 15%, $5 \leq Re \leq 30$, Raschig ring

$s = 0.74\ Re^{0.37}$ max. error 5%, $13 \leq Re \leq 30$, Berl saddle

the effective interfacial area per unit packing volume, a (cm^2/cm^3)

$a = 0.35\ Re^{0.57}$ max. error 5%, $5 \leq Re \leq 30$, Raschig ring

$a = 0.25\ Re^{0.61}$ max. error 10%, $13 \leq Re \leq 30$, Berl saddle

and the mass transfer coefficient of CO_2 absorption into glycerine-water solution

$$\frac{k_L * a}{D} = 1.55\ Re^{0.72}\ Sc^{0.5}$$ max. error 20%

for $20 \leq Re \leq 130$ and $525 \leq Sc \leq 3390$.

Discussion of Results

There have been many investigations concerning gas absorption in a packed tower. The goals of these investigations have been to determine the mass transfer coefficient and the effective interfacial area. These investigations have usually been performed using the two-step procedure. The first step is to obtain the mass transfer coefficient in an apparatus with known contacting area, like a stirred cell reactor or a rotation drum. The second step is to absorb the same gaseous component within a packed tower to obtain the interfacial area for the given packing using the mass transfer coefficient obtained in the previous step.

Danckwerts developed the method to obtain the mass transfer coefficient and effective interfacial area simultaneously in a one-step experiment[4]. He explained the method with his surface renewal theory[2] and obtained the surface renewal rate, s, and the effective interfacial area, a, for a concurrent tower packed with ½-inch Raschig rings[5]. This is the first and only reported investigation of the surface renewal rate for a packed tower.

The values of surface renewal rate, s, obtained by Danckwerts using a concurrent packed tower are plotted in Figure 27 to compare with those obtained in this experiment. As can be seen in this figure, the surface renewal rates, s, obtained in this study have smaller values than those of Danckwerts' study.

The values of the effective interfacial area per unit packing volume, a, for gas absorption with simultaneous chemical reaction, which were obtained in this study, are plotted in Figure 28 together with the plot of data from Danckwerts' research. The values of the effective interfacial obtained in this study is larger than those of Danckwerts. Based upon equation(26), one would expect lower values of the interfacial area, a, when higher values of surface renewal rate, s, are used to determine it.

To determine why there is a discrepancy between Danckwerts' reported values of the interfacial area per unit packing volume, a, and the values reported in this investigation, one must consider the differences in the two packed tower investigations. First, Danckwerts' tower packing density was 15% less dense than that used in this study; however, the density of packing used in this study is consistent with that used in industrial towers. Danckwerts' tower involved concurrent flow. Danckwerts assumed that the mass transfer coefficient for gas absorption with fast chemical reaction in a concurrent packed tower should be essentially the same as that in a countercurrent packed tower. This has not been experimentally verified; in fact, the data in this experiment would tend to challenge this conclusion. The third possible cause of the discrepancy may have been due to the different means of distributing the liquid to the top of the packed section. Low values of k_L*a were obtained

in this investigation when a different liquid distributor was used. Unfortunately, scattered data were obtained due to apparent poor liquid distribution within the packing. Accordingly, a new liquid distributor was designed and used to obtain the reported values. The higher value of mass transfer coefficient obtained in this experiment than in Danckwerts' is probably due to the countercurrent flow pattern, denser packing, and what appears to be a more uniform liquid distribution to the packing. See Figure 29.

The surface renewal rate, s, for ½-inch Berl saddles has never been studied previously. Any comparison of this value obtained in this experiment with other research was not possible. The effective interfacial area, a, per unit packing volume for gas absorption with simultaneous chemical reaction in packed tower with ½-inch Berl saddle is plotted in Figure 30 along with a plot of calculated values of the effective area as wetted area predicted by Onda's equation[12]. As can be seen in this figure, the effective interfacial area for gas absorption with simultaneous chemical reaction shows larger values than that of wetted area for physical absorption.

According to the Danckwerts' theory, the liquid mass transfer coefficient for physical absorption could be evaluated by the equation

$$k_L = \sqrt{Ds} \tag{30}$$

and the k_L*a coefficient could be determined using the surface renewal rate, s, and the effective interfacial

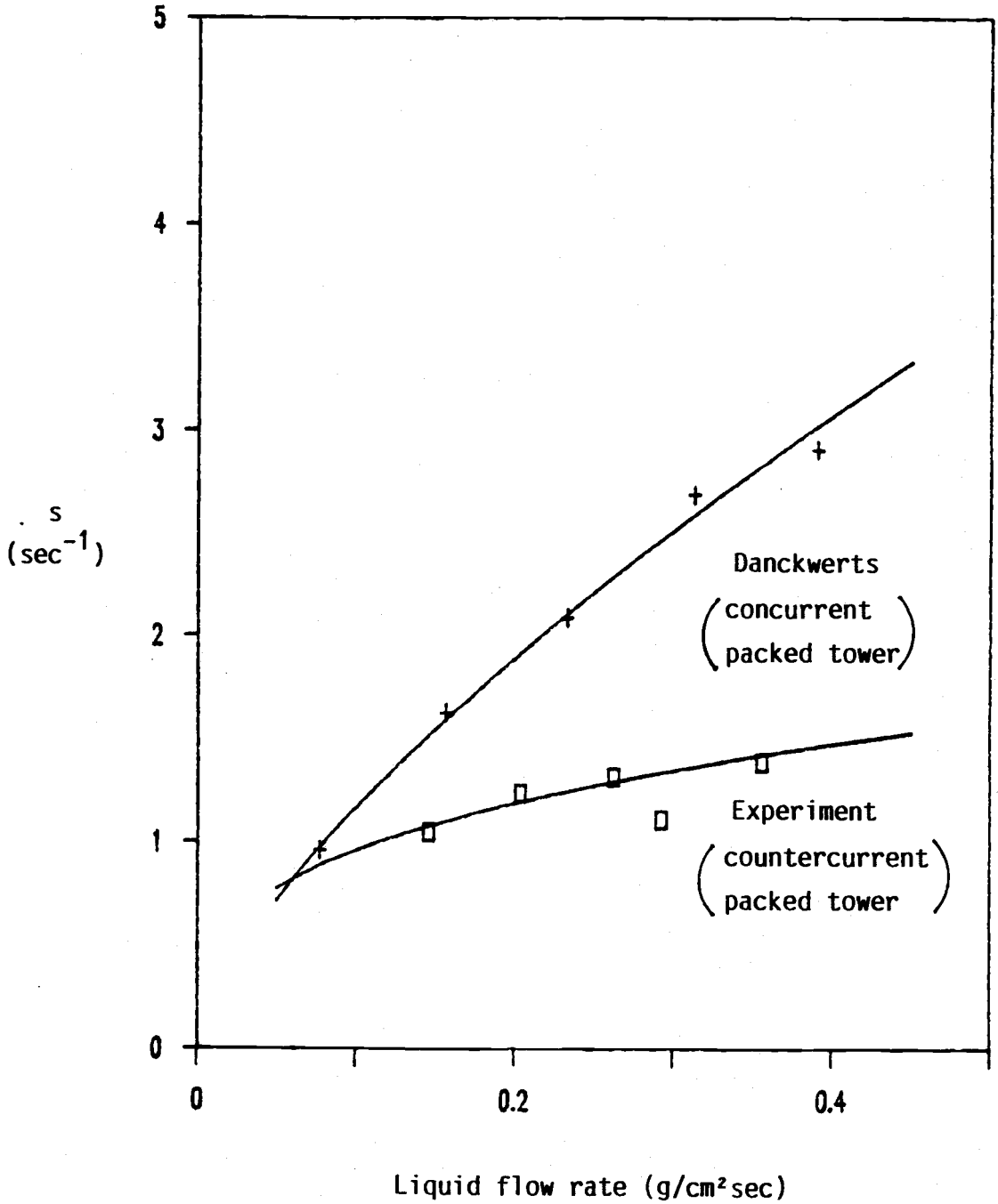

Figure 27. Comparison of s with previous experiment for $\frac{1}{2}$-inch Raschig ring

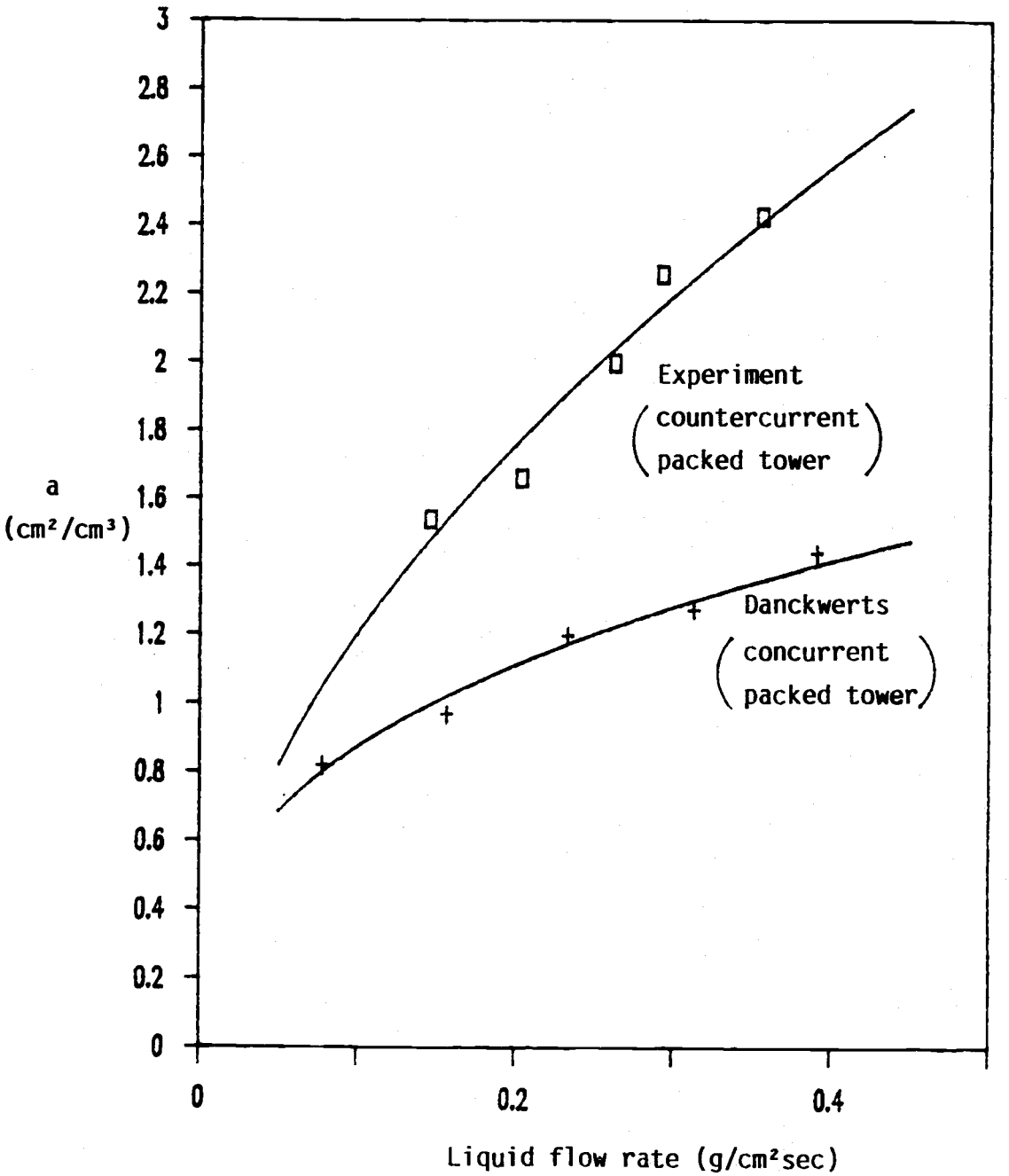

Figure 28. Comparison of areas for ½-inch Raschig ring

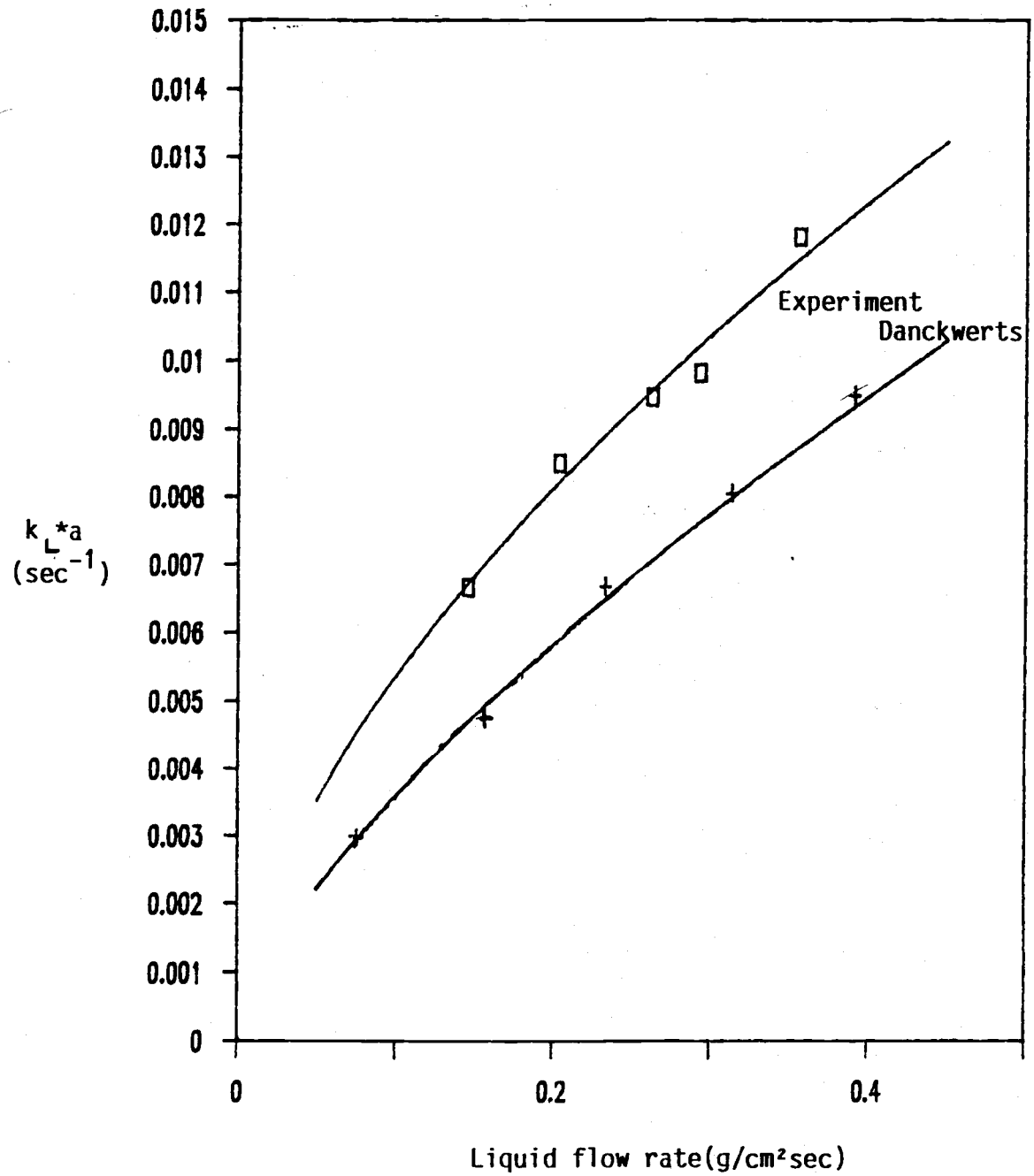

Figure 29. Comparison of mass transfer coefficient with previous researcher's for ½-inch Raschig ring

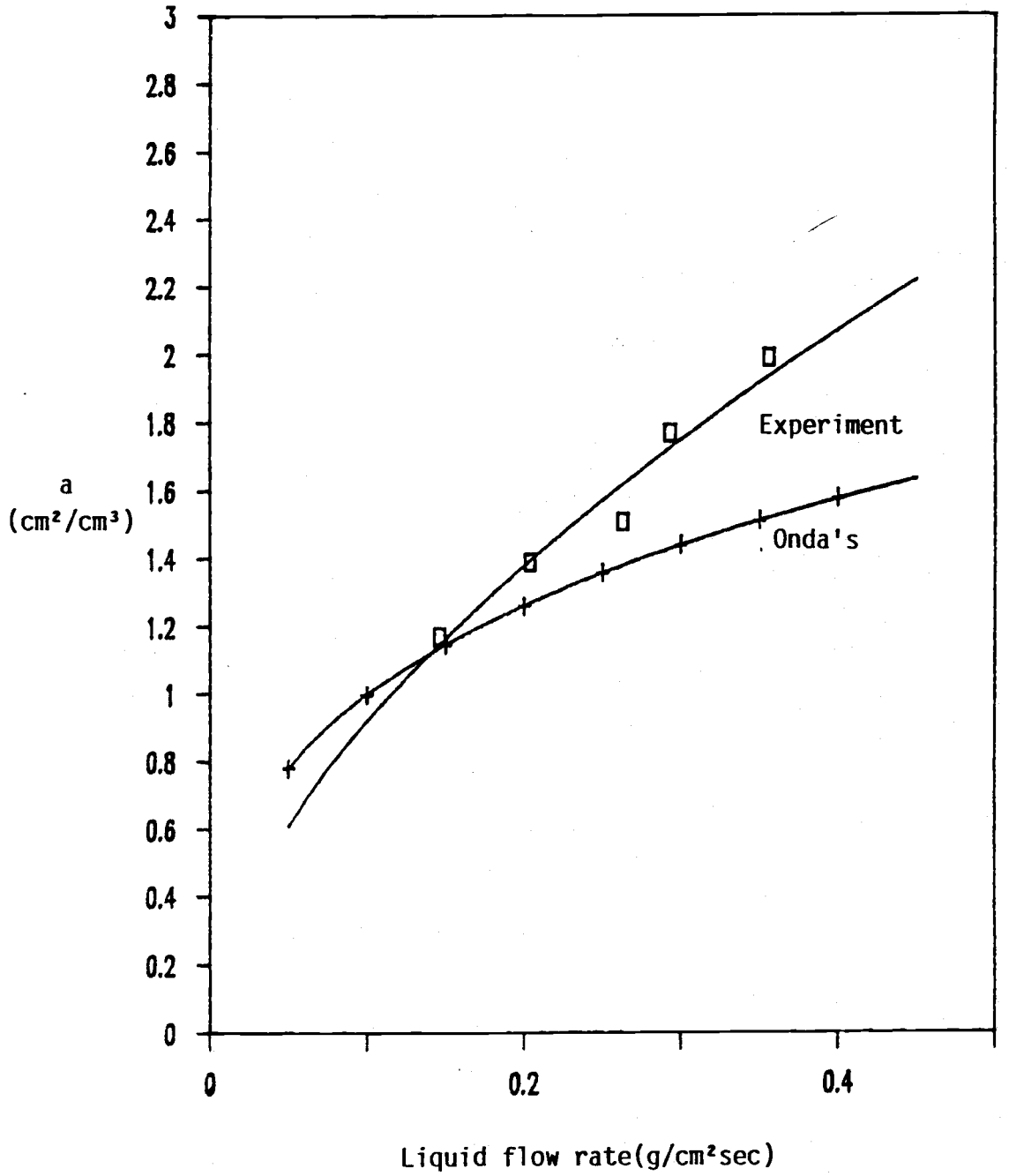

Figure 30. Comparison of a with previous research for ½-inch Berl saddle

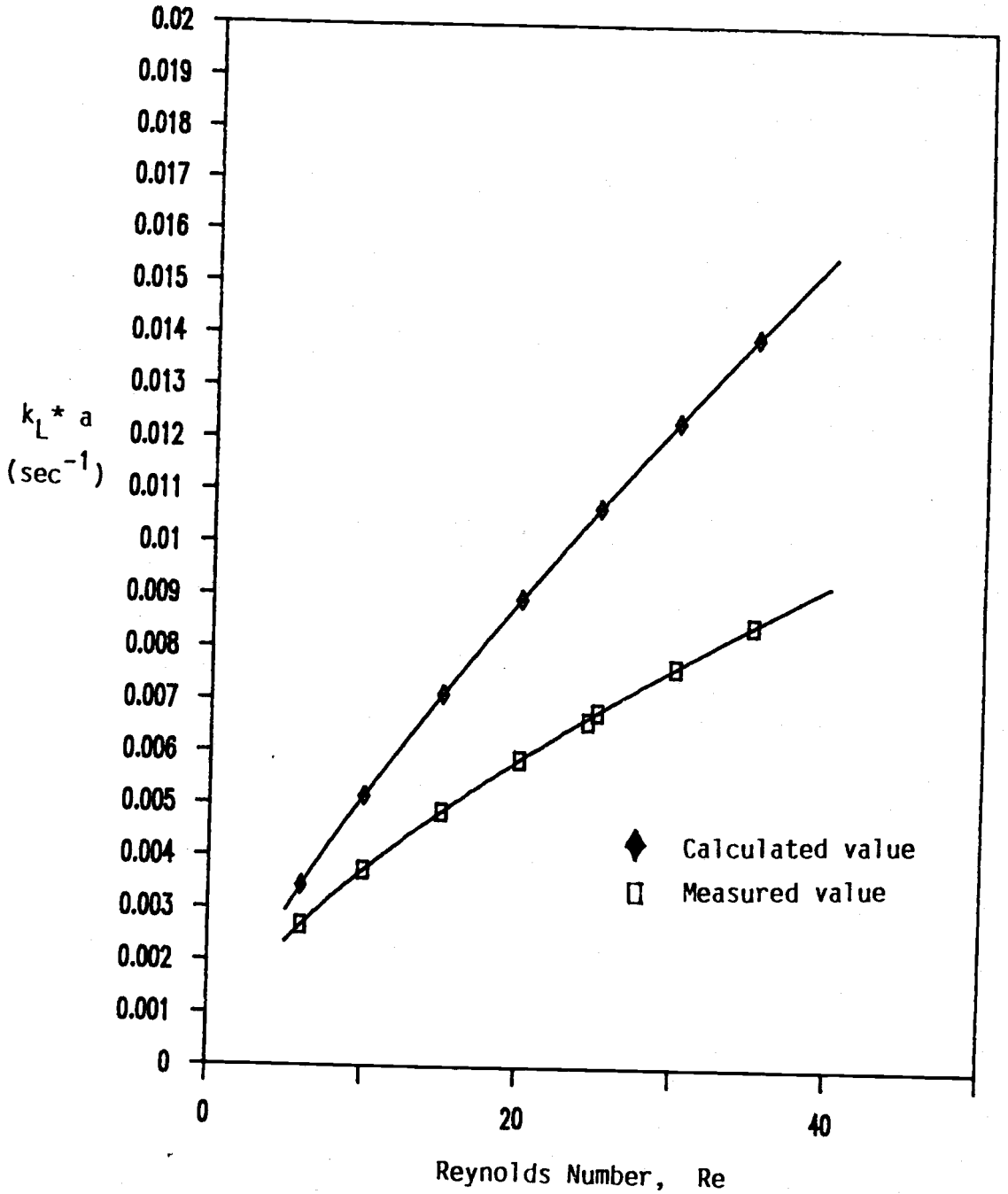

Figure 31. Comparison of calculated value and measured value of mass transfer coefficient of CO_2 absorption into water

area, a, previously established for the given packing and the established Reynolds number. The mass transfer coefficient per unit packing volume for the absorption of CO_2 into water in a packed tower with ½-inch Berl saddles was determined by this method (referred to as calculated values) and compared to the values experimentally measured (referred to as physical absorption values) in Figure 31. As can be seen in this figure, the calculated values from Danckwerts' theory are 50% larger than those experimentally measured. It is assumed to be due to the increase of the absorption capacity of buffer solution from which the values of surface renewal rate and the effective interfacial area were obtained[28]. Because of the increased capacity and the rate of absorption due to chemical reaction, a slowly moving portion of liquid still remains active in absorption and reaction. Otherwise, this portion of liquid will be saturated soon after contacting the gas. This portion of fluid may be supposed to increase the mass transfer coefficient per unit packing volume in the packing section.

Conclusions

After examining the results from this experiment and comparing them with previous investigations, the author came to following conclusions:

(1) The surface renewal rate, s, in the packed tower can be expressed as a function of the Reynolds number. Since this investigation involved varying the liquid velocity only, future simultaneous absorption with chemical reaction studies involving other fluid properties need to be conducted.

(2) Countercurrent operations, denser packing arrangements, and an apparently more uniform distribution of liquid over the packing section make the mass transfer coefficient larger than that obtained by Danckwerts.

(3) The investigations of gas absorption into various viscous fluid elucidate the relationships between the mass transfer coefficient per unit volume and liquid properties.

(4) Comparison of the mass transfer coefficient calculated from Danckwerts' theory and the measured values from gas absorption into water shows that the values obtained from Danckwerts' theory are larger than measured ones due to the buffer solution's increased capacity of absorption of CO_2.

The following investigations are suggested for a clearer understanding of the mechanism of gas absorption with chemical reaction in a packed tower.

(1) Adequate reaction kinetics data are necessary to

perform gas absorption with chemical reaction into glycerine-water buffer solution; with these data, further research should be conducted on the influence of density and viscosity on the surface renewal rate, s, and the effective interfacial area, a. The physical absorption investigation revealed a definite effect as the glycerine concentration (thus density and viscosity) changes. Accordingly, one would expect these variables to have an effect on the s and a values.

(2) Since there were discrepancies between the concurrent flow data of Danckwerts and the countercurrent flow data of this experiment, further research should be conducted to determine why these discrepancies exist. One might hypothesize that it was due to the mixing action which may have possibly changed both the interfacial area and the rate of surface renewal.

(3) Further investigations of the Danckwerts' one-step method for evaluating the interfacial area, a, and the surface renewal rate, s, for other types of operating systems should be done. This will require both kinetics and mass transfer data.

Notations

a : effective interfacial area per unit packing volume [cm^2/cm^3]

c : concentration of solute in solution [$gmol/cm^3$]

c^* : saturated concentration in solution [$gmol/cm^3$]

c_w : saturated concentration in water [$gmol/cm^3$]

D : diffusion coefficient [cm^2/sec]

D_w : diffusion coefficient in water [cm^2/sec]

k_1 : pseudo-first order reaction rate constant [sec^{-1}]

k_L : mass transfer coefficient [cm/sec]

L : liquid flow rate per unit cross area of packing section [g/cm^2sec]

N : solute transfer rate across an unit area of interface [$gmol/cm^2sec$]

Re : Reynolds number [D_pL/μ]

s : surface renewal rate [sec^{-1}]

Sc : Schmidt number of liquid solution [$\mu/\rho D$]

Greek

δ : film thickness for film theory [cm]

μ : viscosity of liquid solution [g/cmsec]

ρ : density of liquid solution [g/cm^3]

ã : constant in equation for s

ß : constant in equation for a

γ : constant in equation(53)

Literature cited

[1] Danckwerts, P. V., Ind. Eng. Chem., **43**, 1460 (1951).

[2] Danckwerts, P. V., A. M. Kennedy, Trans. Instn. Chem. Engrs., **32**, S49 (1954).

[3] Danckwerts, P. V., A. M. Kennedy, Trans. Instn. Chem. Engrs., **32**, S53 (1954).

[4] Danckwerts, P. V., A. M. Kennedy, Chem. Eng. Sci., **17**, 961 (1962).

[5] Richards, G. M., G. A. Ratcliff, P. V. Danckwerts, Chem. Eng. Sci., **19**, 325 (1964).

[6] Danckwerts, P. V., Gas-Liquid Reactions, McGraw-Hill, New York, (1970).

[7] Shah, Y. T., Gas-Liquid-Solid Reactor Design, McGraw-Hill, New York, (1979).

[8] NATO ASI Series, Mass Transfer with Chemical Reaction in Multiphase Systems, Series E, No.72, Martinus Nijhoff Publishers, The Hague, (1983).

[9] Ramm, V. M., Absorption of Gases, Israel Program for Scientific Translation, Jerusalem, (1968).

[10] Sherwood, T. K., F. A. L. Holloway, Trans. Am. Inst. Chem. Engrs., **35**, 39 (1950).

[11] Mangers, R. J., A. B. Ponter, Ind. Eng. Chem. Process Des. Dev., **19**, 530 (1980).

[12] Onda, K., H. Takeuchi, Y. Koyama, Kagaku Kogaku, **31**, 126 (1967).

[13] Semmelbauer,R., Chem. Eng. Sci., **22**, 1237 (1967).

[14] Sharma, M. M., P. V. Danckwerts, Brit. Chem. Eng., **15**, 522 (1970).

[15] Lewis, W. K., W. G. Whitman, Ind. Eng. Chem., **16**, 1215 (1924).

[16] Higbie, R., Trans. Am. Inst. Chem. Engrs., **31**, 365 (1935).

[17] Levich, V. G., Physicochemical Hydrodynamics, Prentice- Hall, Englewood Cliffs, N. J., (1962).

[18] Sherwood, T. K., J. M. Ryan, Chem. Eng. Sci., **11**, 81 (1959).

[19] Ruckenstein, E., Chem. Eng. Sci., **17**, 265 (1958).

[20] Kishinevskii, M. Kh., A. V. Pamfilov, Zh. Prik. Khimii, **22**, 1173 (1949).

[21] Toor, H. L., J. M. Marcello, A.I.Ch.E. Journal, **4**, 97 (1958).

[22] Pinsent, B. R. W., L. Pearson, F. J. W. Roughton, Trans. Faraday Soc., **52**, 1512 (1956).

[23] Van Klevelen, D. W., P. J. Hoftijzer, Chem. Eng. Prog., **44**, 529 (1948).

[24] Shulman, H. L., C. F. Ulrich, A. Z. Proulx, J. O. Zimmerman, A.I.Ch.E. Journal, **1**, 253 (1955).

[25] Nysing, R. A. T. O., H. Kramers, Chem. Eng. Sci., **8**, 81, (1958).

[26] Hikita, H., S. Asai, T. Takatsuka, The Chem. Eng. Journal, **11**, 131 (1976).

[27] Brignole, E. A., R. Echarte, Chem. Eng. Sci., **36**, 695 (1981).

[28] Joosten, G. E. H., P. V. Danckwerts, Chem. Eng. Sci., 28, 453 (1973).

[29] Astarita, G., Mass Transfer with Chemical Reaction, Elsevier Publishing Co., Amsterdam, 1967.

[30] Sherwood, T. K., R. L. Pigford, C. R. Wilke, Mass Transfer, McGraw-Hill, New York, 1975.

Appendices

Appendix I.

Preparation of Analyzing Solutions

(1) 1N NaOH solution - This solution was made of 40 g NaOH in 1 liter solution. 40g of NaOH was weighted precisely and put into a 1 liter mass flask to make 1 liter solution by adding distilled water. Around 3 grams of oxalic acid ($H_2C_2O_4.2H_2O$) was weighted exactly to ±0.1 mg and dissolved into 200 cm^3 water. This oxalic acid solution has very accurate normality and can be used as a standard solution to determine the concentration of the other basic solution. This solution was titrated by NaOH solution made in the previous step with 2-3 drops of phenolphthalein solution as an indicator. This titration will give the exact concentration of NaOH solution. NaOH solution will make carbonate precipitation around the cap of the bottle by a reaction with CO_2 in the air, causing the cap to be stuck to the bottle. Accordingly, a plastic bottle cap should be used to prevent sticking.

(2) 1 N HCl solution - 81 cm^3 of concentrated HCl solution (12 N) was diluted into 1 N HCl solution (volume 1 liter). This solution was titrated to determine the normality with 1 N NaOH solution of which the concentration was determined in the previous step. 2-3 drops of phenolphthalein was used as an indicator.

(3) 1 N oxalic acid solution - 63.1 gram of oxalic acid powder was dissolved into 1 liter solution to make 1 N acid solution. The determination of the concentration of this solution is the same as that of HCl solution.

(4) 1 N $BaCl_2$ solution - 244.28 gram of $BaCl_2$ was

dissolved into water to make 1 liter of 1 N $BaCl_2$ solution. This solution's concentration need not to be known as accurately as the previous titrating solution.

(5) Phenolphthalein solution - 100 mg of phenolphthalein powder dissolved into 100 gram of 60% methanol- water mixture. For this indicator, the range of color change is ph 8.3-10.0. This solution was used for the titration of total concentration of OH^- with oxalic acid.

(6) Methyl red solution - 200 mg of methyl red powder was dissolved into 100 gram of 90% methanol solution. The range of color change is ph.4.4 to 6.2 and the color in acid is yellow and it changes to red in base.

Appendix II.

Physical properties of Glycerine-water Solution

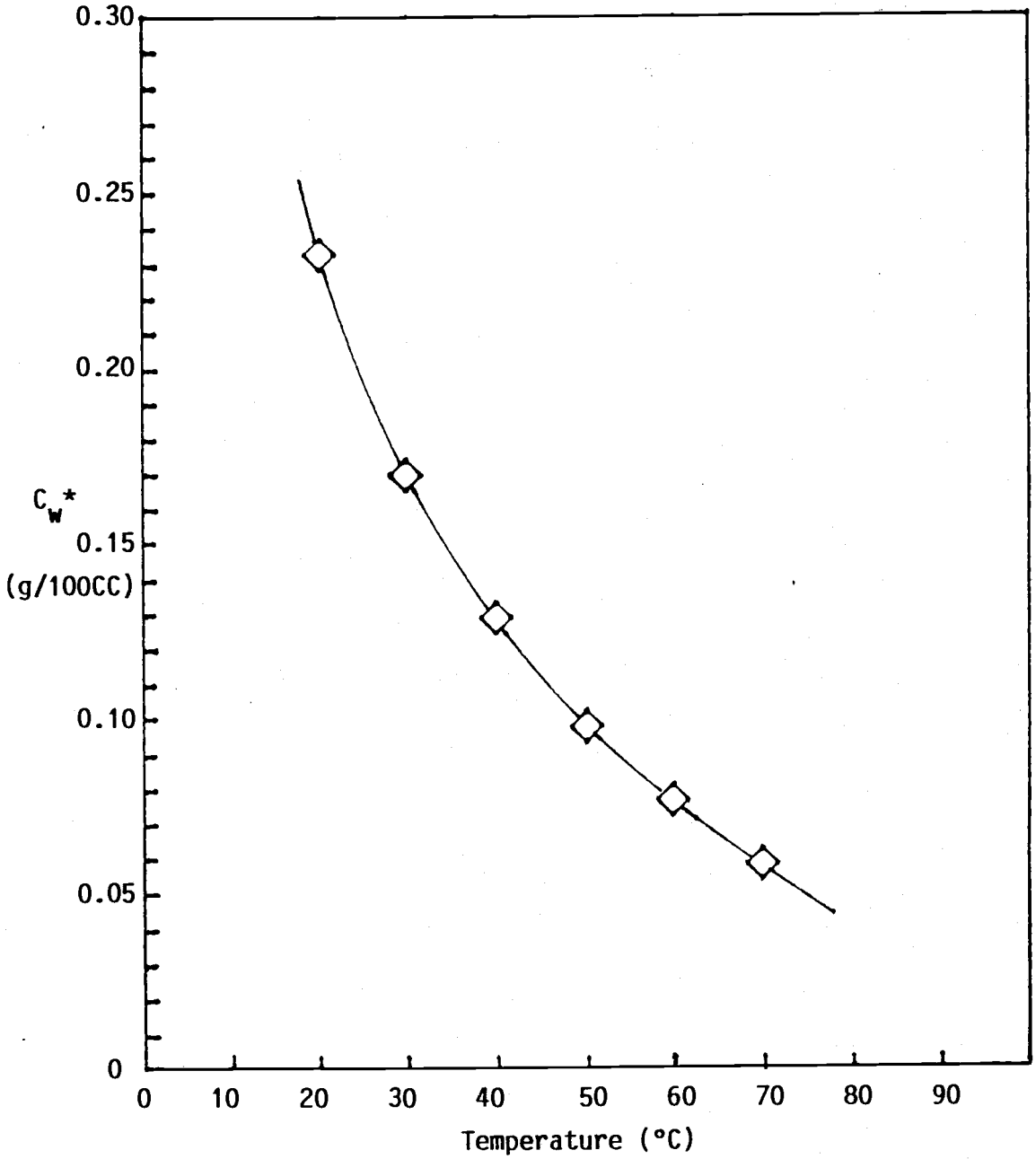

Figure 32 . Solubility of CO_2 in water at p=1 atm

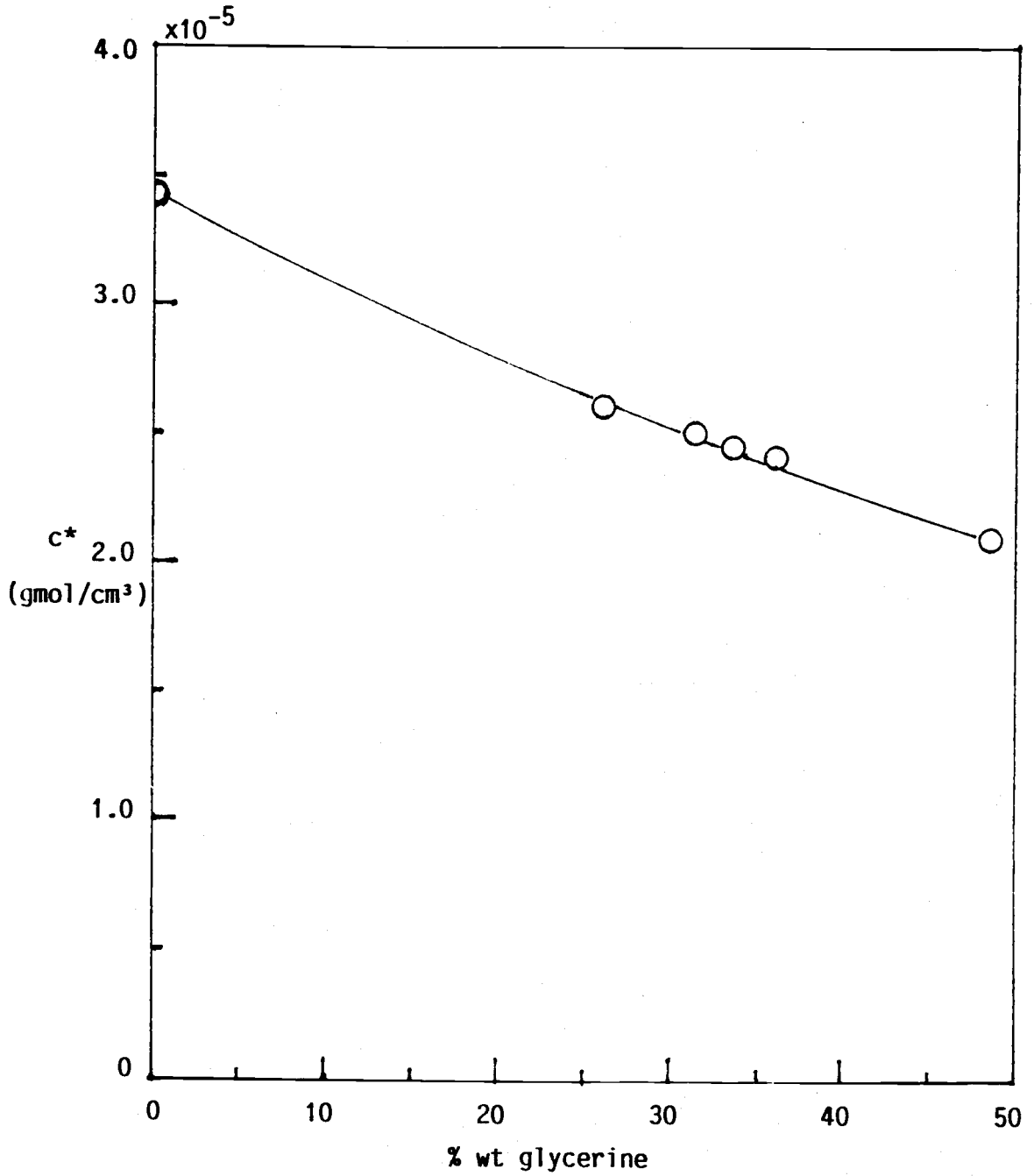

Figure 33. Solubility of CO_2 in glycerine-water solution at 25°C

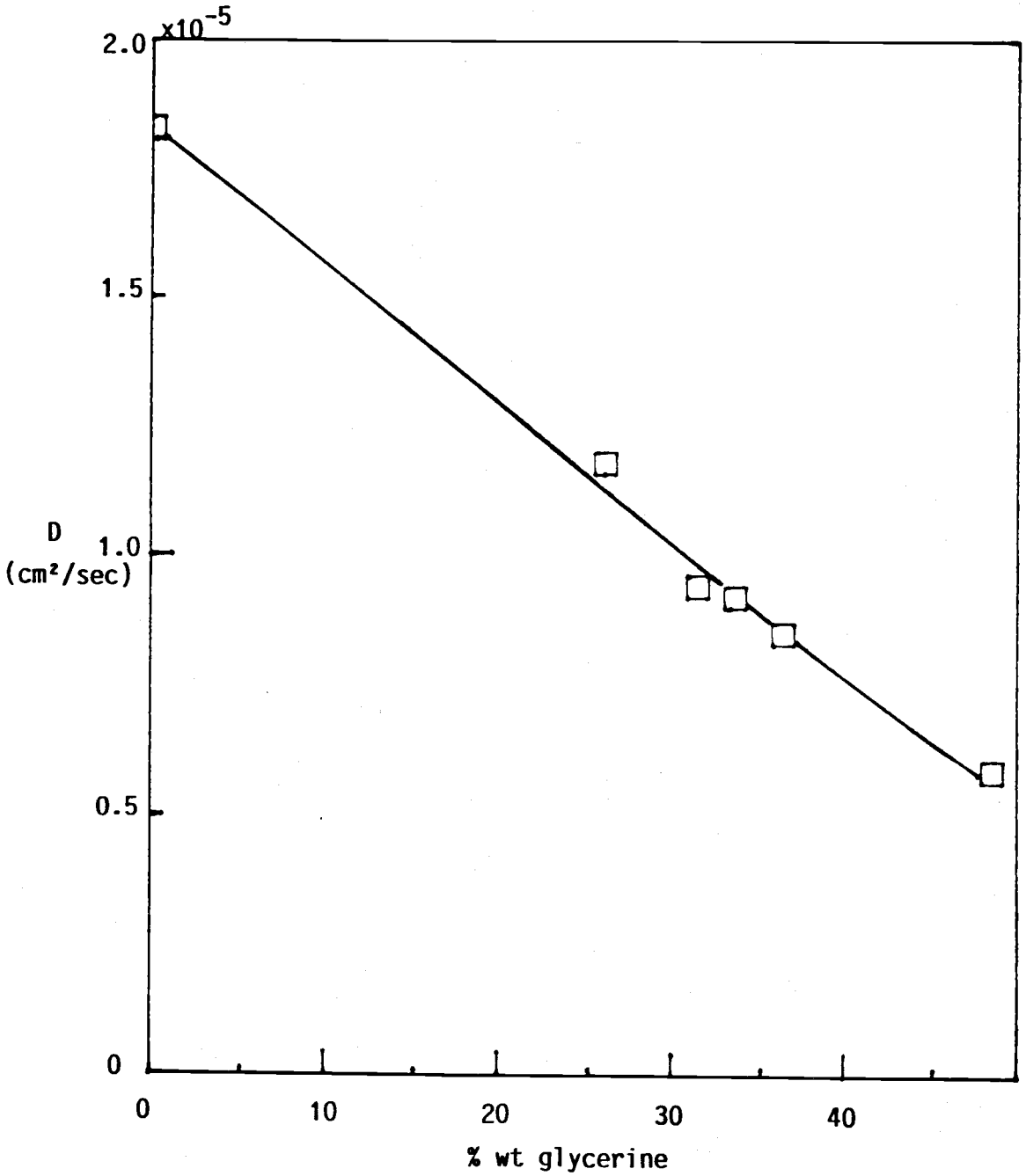

Figure 34 . Mass diffusity of CO_2 in glycerine-water solution at 25°C

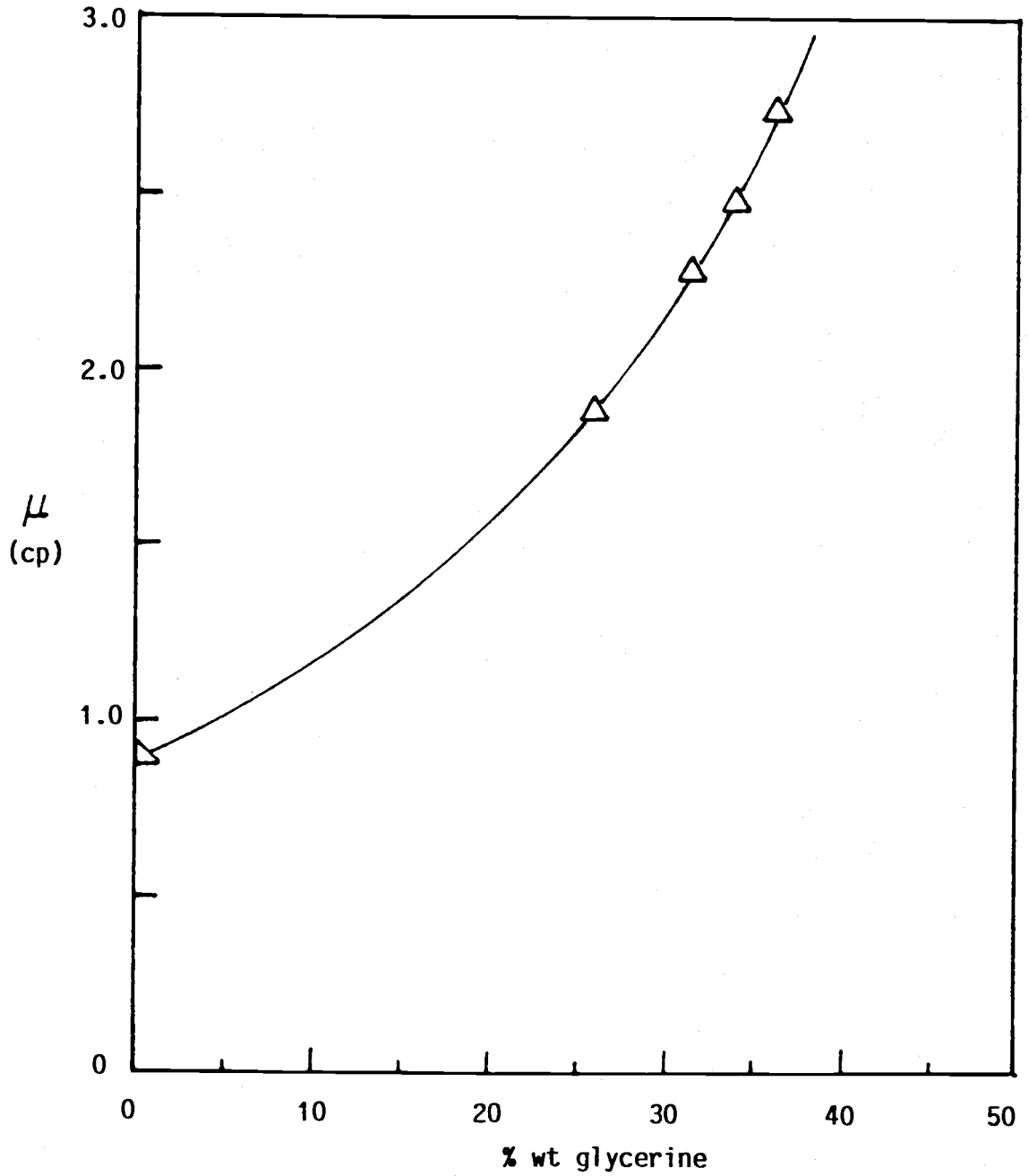

Figure 35. Viscosity of glycerine-water solution at 25°C

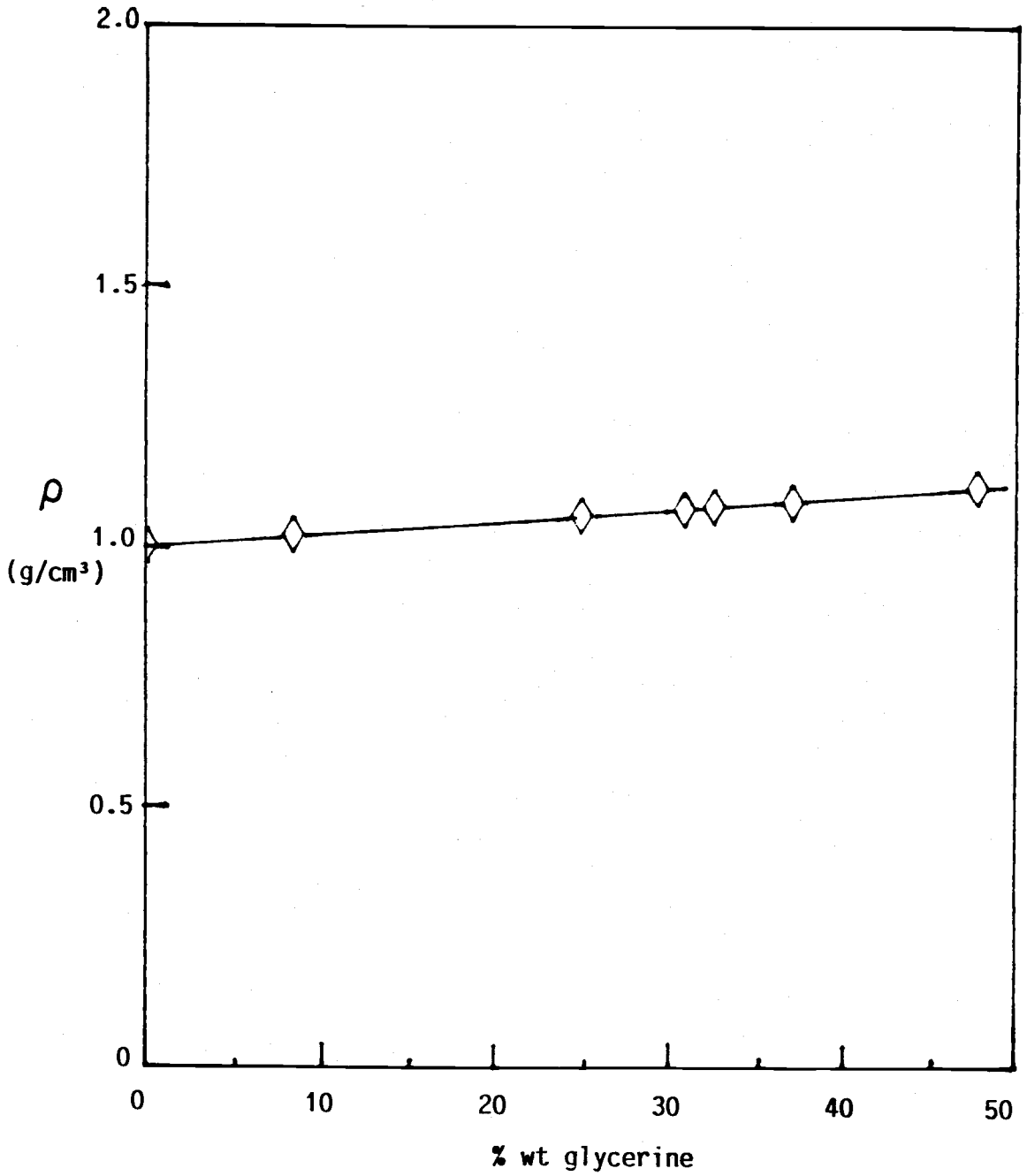

Figure 36. Density of glycerine-water solution at 25°C

Appendix III.

Calibration Curves of Rotameters

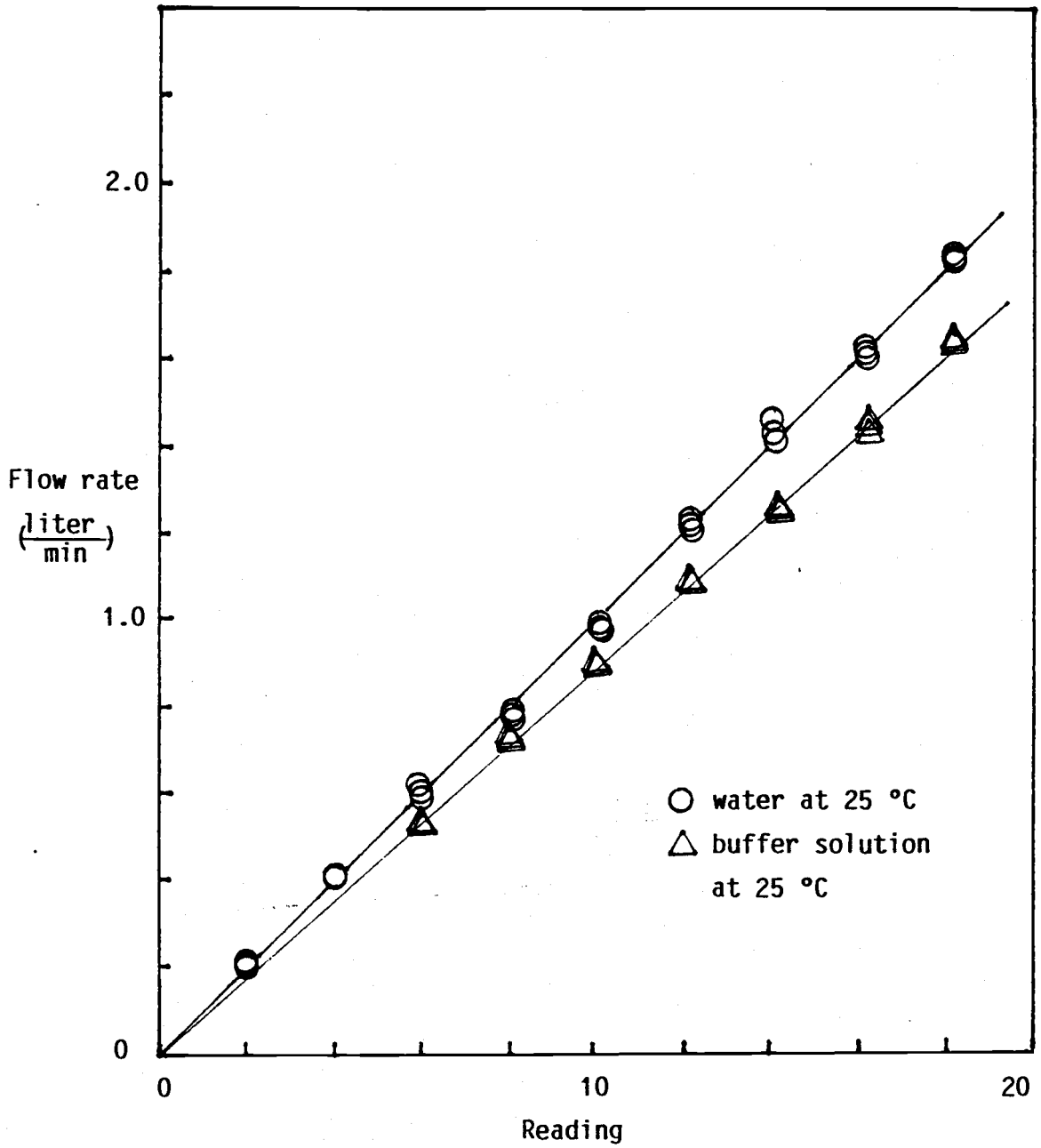

Figure 37. Calibration curve for buffer solution

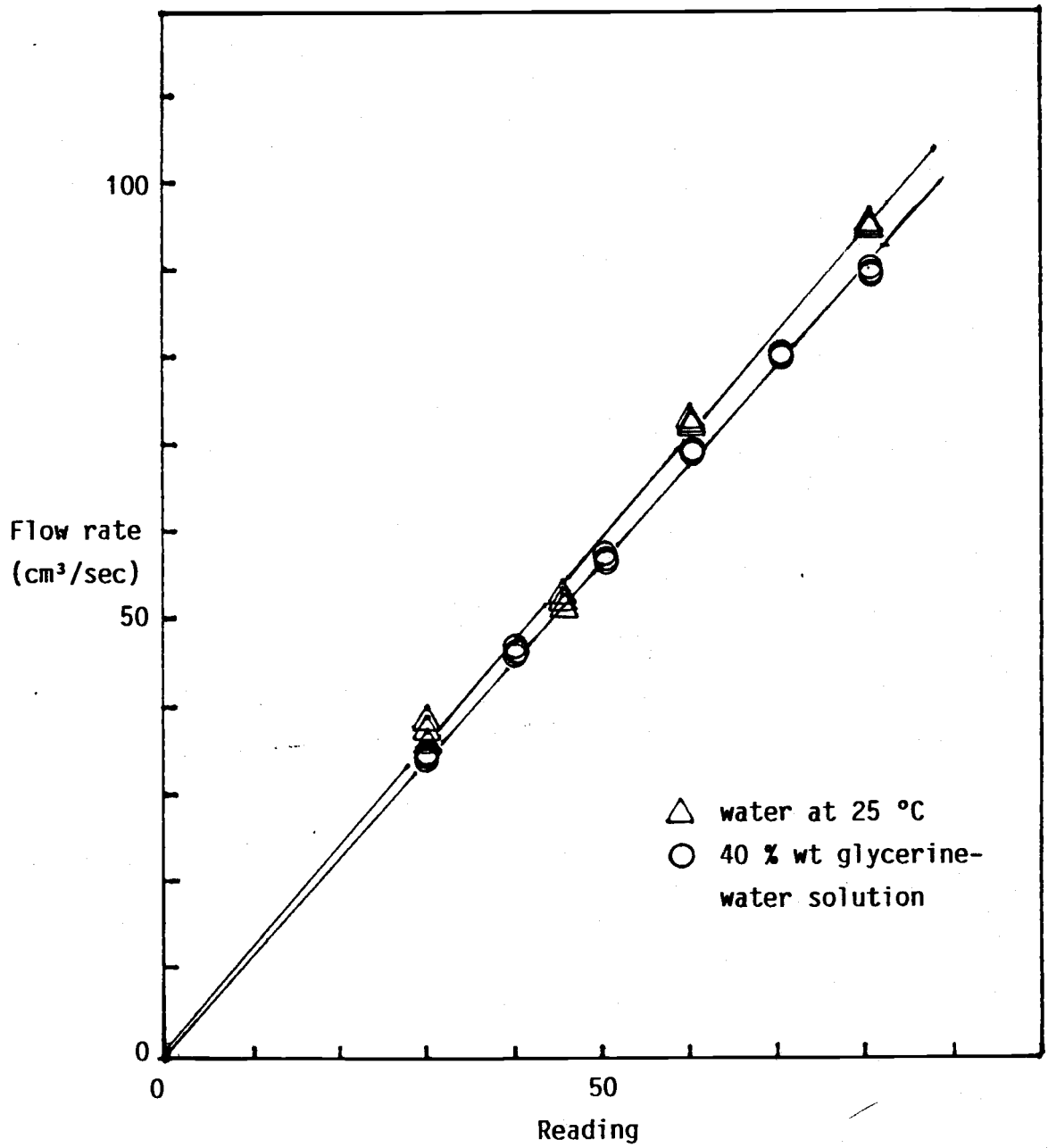

Figure 38. Calibration curve for glycerine-water solution

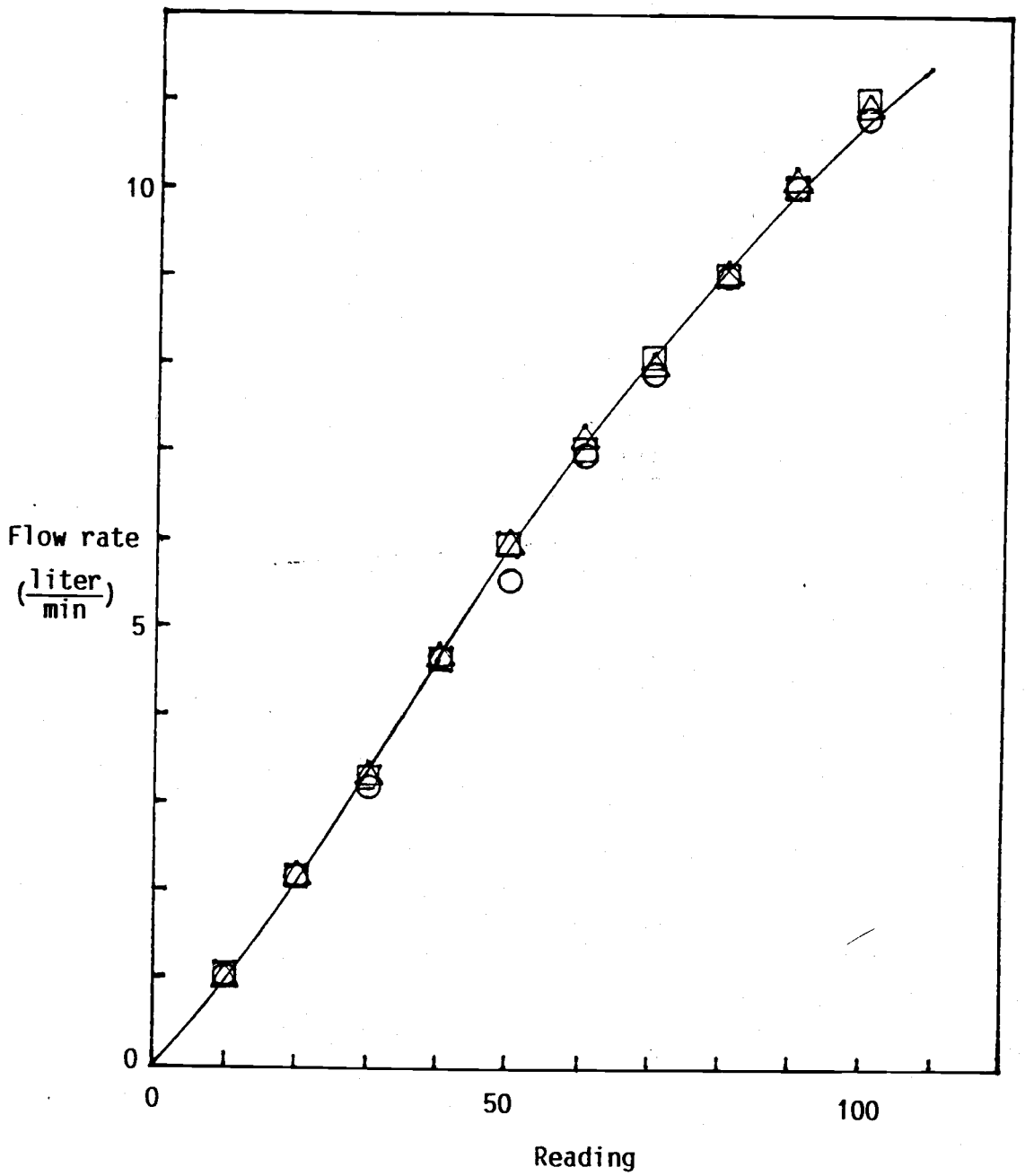

Figure 39. Calibration curve for air at 25°C, 1 atm

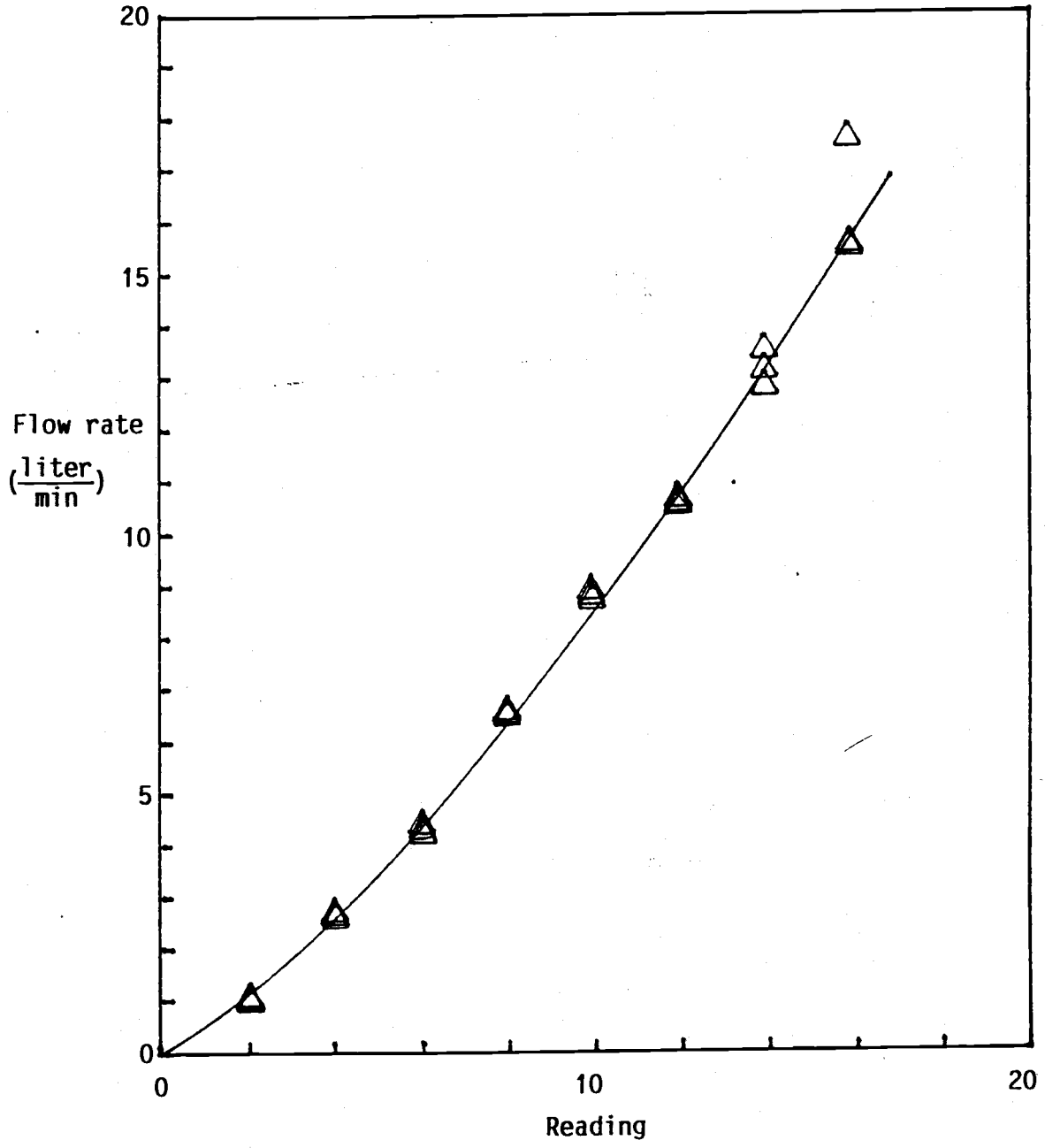

Figure 40. Calibration curve of air at 25 °C, 1 atm

Appendix IV

Tables of experimental data

Table IV-a. Table of experimental data for ½-inch Raschig ring

G = 300 cm^3/sec of CO_2 at 1 atm, 25°C

liquid flow g/cm^2s	initial $[HCO_3^-]$ gmol/l	initial $[CO_3^{-2}]$ gmol/l	buffer ratio	k_l sec^{-1}	final $[HCO_3^-]$ gmol/l	$(N*a)x10^7$ $gmol/cm^3s$
0.146	0.756	0.527	0.63	0.54	0.829	1.487
0.146	0.817	0.561	0.70	0.60	0.923	1.640
0.146	0.514	0.632	0.925	0.78	0.639	1.679
0.146	0.426	0.713	1.395	1.15	0.525	1.879
0.146	0.348	0.760	2.38	1.91	0.434	2.027
0.146	0.247	0.808	2.78	2.21	0.378	2.369
0.204	0.641	0.505	0.73	0.62	0.698	1.851
0.204	0.601	0.525	0.81	0.69	0.669	1.879
0.204	0.550	0.551	0.93	0.79	0.613	2.059
0.204	0.485	0.583	1.12	0.94	0.554	2.257
0.204	0.434	0.609	1.31	1.09	0.507	2.393
0.204	0.319	0.666	1.94	1.57	0.395	2.459
0.204	0.214	0.719	2.75	2.19	0.294	2.616
0.263	0.742	0.381	0.46	0.40	0.802	2.003
0.263	0.587	0.550	0.89	0.75	0.642	2.256
0.263	0.538	0.574	1.02	0.85	0.594	2.326
0.263	0.394	0.684	1.59	1.30	0.456	2.575
0.263	0.283	0.740	2.37	1.90	0.351	2.884
0.263	0.200	0.743	2.90	2.30	0.269	2.934
0.293	0.621	0.572	0.85	0.72	0.672	2.369
0.293	0.558	0.603	0.95	0.80	0.610	2.425
0.293	0.454	0.655	1.36	1.12	0.512	2.707
0.293	0.369	0.668	1.74	1.42	0.422	2.472
0.293	0.313	0.696	2.08	1.68	0.376	2.910
0.293	0.298	0.733	2.33	1.87	0.366	3.177
0.293	0.272	0.717	2.38	1.91	0.337	3.304
0.293	0.209	0.734	2.90	2.30	0.286	3.572
0.356	0.618	0.596	0.92	0.87	0.665	2.678
0.356	0.567	0.621	0.98	0.82	0.617	2.862
0.356	0.527	0.641	1.21	1.00	0.579	2.953
0.356	0.482	0.663	1.36	1.12	0.535	3.015
0.356	0.208	0.766	1.50	1.23	0.281	3.063
0.356	0.392	0.709	1.84	1.50	0.446	3.089
0.356	0.288	0.715	2.24	1.80	0.369	3.526
0.356	0.426	0.711	2.93	2.32	0.487	3.684

Table IV-b. Table of experimental data for ½-inch Berl saddle

G = 300 cm^3/sec of CO_2 at 1 atm, 25°C

liquid flow g/cm^2s	initial $[HCO_3^-]$ gmol/l	initial $[CO_3^{-2}]$ gmol/l	buffer ratio	k_l sec^{-1}	final $[HCO_3^-]$ gmol/l	$(N*a)x10^7$ $gmol/cm^3s$
0.146	0.63	0.532	0.77	0.66	0.699	1.444
0.146	0.577	0.561	0.89	0.75	0.653	1.702
0.146	0.522	0.588	1.04	0.87	0.601	1.769
0.146	0.496	0.615	1.22	1.02	0.546	1.721
0.146	0.399	0.650	1.52	1.25	0.480	1.792
0.146	0.334	0.683	1.89	1.53	0.415	1.817
0.146	0.282	0.709	2.24	1.81	0.366	1.883
0.204	0.668	0.519	0.53	0.61	0.727	1.843
0.204	0.617	0.544	0.82	0.70	0.677	1.868
0.204	0.563	0.571	0.95	0.80	0.627	2.009
0.204	0.506	0.600	1.11	0.93	0.573	2.099
0.204	0.452	0.627	1.33	1.09	0.514	1.945
0.204	0.245	0.730	2.58	2.06	0.319	2.316
0.263	0.631	0.535	0.79	0.67	0.685	2.165
0.263	0.581	0.560	0.90	0.76	0.639	2.314
0.263	0.434	0.634	1.43	1.18	0.497	2.545
0.263	0.327	0.688	1.98	1.60	0.392	2.611
0.263	0.278	0.712	2.34	1.88	0.343	2.644
0.263	0.222	0.740	2.78	2.21	0.290	2.760
0.293	0.564	0.556	0.92	0.78	0.620	2.502
0.293	0.524	0.576	1.04	0.87	0.583	2.630
0.293	0.482	0.597	1.18	0.98	0.541	2.667
0.293	0.433	0.622	1.37	1.13	0.494	2.722
0.293	0.387	0.645	1.60	1.31	0.449	2.778
0.293	0.277	0.700	2.32	1.86	0.343	2.980
0.293	0.220	0.728	2.77	2.20	0.288	3.053
0.356	0.617	0.569	0.78	0.66	0.669	2.799
0.356	0.474	0.641	1.29	1.07	0.530	3.068
0.356	0.429	0.664	1.50	1.23	0.486	3.112
0.356	0.386	0.685	1.72	1.40	0.443	3.157
0.356	0.331	0.713	2.06	1.66	0.390	3.224

Table IV-c. Table of experimental data for glycerine-water solution

G = 300 cm^3/sec of CO_2 at 1 atm, 25°C

% wt of glycerine	liquid flow cm^3/sec	Final concentration of CO_2 gmol/liter	$(N*a)X10^7$ gmol/cm^3s
0	14	2.631	1.385
0	27	2.213	2.329
0	38	2.090	3.097
0	49	1.989	3.801
0	61	1.840	4.377
0	72	1.705	4.785
10	14	2.038	1.072
10	26	1.772	1.797
10	38	1.639	2.364
10	49	1.534	2.810
10	60	1.310	3.039
10	71	1.251	3.463
20	13	1.586	0.804
20	26	1.378	1.397
20	37	1.330	1.892
20	48	1.242	2.300
20	59	1.172	2.696
20	71	1.117	3.071
30	13	1.464	0.713
30	25	1.293	1.260
30	36	1.146	1.563
30	47	0.964	1.729
30	58	0.789	2.091
30	70	0.938	2.541
30	81	0.859	2.695
30	91	0.832	2.953
40	12	1.293	0.605
40	24	1.161	1.086
40	35	0.968	1.321
40	46	0.881	1.579
40	58	1.000	2.264
40	69	0.744	1.974
40	80	0.806	2.514
40	90	0.651	2.283